Fundamental Research 4 (2024) 806–819

Contents lists available at ScienceDirect

Fundamental Research

journal homepage: http://www.keaipublishing.com/en/journals/fundamental-research/

Article

Activation and polarization of striatal microglia and astrocytes are involved in bradykinesia and allodynia in early-stage parkinsonian mice

Xue Zhang [a], Zi-Lin Shen [a], Ya-Wei Ji [a], Cui Yin [a,b,c], Cheng Xiao [a,b,c,*], Chunyi Zhou [a,b,c,*]

[a] Jiangsu Province Key Laboratory of Anesthesiology, School of Anesthesiology, Xuzhou Medical University, Xuzhou 221004, China
[b] Jiangsu Province Key Laboratory of Anesthesia and Analgesia Application Technology, Xuzhou Medical University, Xuzhou 221004, China
[c] NMPA Key Laboratory for Research and Evaluation of Narcotic and Psychotropic Drugs, School of Anesthesiology, Xuzhou Medical University, Xuzhou 221004, China

ARTICLE INFO

Article history:
Received 20 October 2022
Received in revised form 13 April 2023
Accepted 17 May 2023
Available online 16 July 2023

Keywords:
Parkinson's disease
Dopaminergic system
Striatum
Microglia
Astrocytes
Substantia nigra pars compacta

ABSTRACT

In addition to the cardinal motor symptoms, pain is a major non-motor symptom of Parkinson's disease (PD). Neuroinflammation in the substantia nigra pars compacta and dorsal striatum is involved in neurodegeneration in PD. But the polarization of microglia and astrocytes in the dorsal striatum and their contribution to motor deficits and hyperalgesia in PD have not been characterized. In the present study, we observed that hemiparkinsonian mice established by unilateral 6-OHDA injection in the medial forebrain bundle exhibited motor deficits and mechanical allodynia. In these mice, both microglia and astrocytes in the dorsal striatum were activated and polarized to M1/M2 microglia and A1/A2 astrocytes as genes specific to these cells were upregulated. These effects peaked 7 days after 6-OHDA injection. Meanwhile, striatal astrocytes in parkinsonian mice also displayed hyperpolarized membrane potentials, enhanced voltage-gated potassium currents, and dysfunction in inwardly rectifying potassium channels and glutamate transporters. Systemic administration of minocycline, a microglia inhibitor, attenuated the expression of genes specific to M1 microglia and A1 astrocytes in the dorsal striatum (but not those specific to M2 microglia and A2 astrocytes), attenuated the damage in the nigrostriatal dopaminergic system, and alleviated the motor deficits and mechanical allodynia in parkinsonian mice. By contrast, local administration of minocycline into the dorsal striatum of parkinsonian mice mitigated only hyperalgesia. This study suggests that M1 microglia and A1 astrocytes in the dorsal striatum may play important roles in the development of pathophysiology underlying hyperalgesia in the early stages of PD.

1. Introduction

Parkinson's disease (PD) is a common neurodegenerative disease affecting more than 6 million patients worldwide [1]. The manifestation of PD includes not only the cardinal motor symptoms of tremor, rigidity, bradykinesia, postural instability, freezing of gait, etc., but also non-motor symptoms such as chronic pain [2,3]. Chronic pain is reported in 40% to 85% of PD patients and seriously affects quality of life [4,5], but the underlying mechanisms remain largely unknown [6]. The loss of dopaminergic (DA) neurons in the substantia nigra pars compacta (SNc) and presence of Lewy body inclusions in the remaining SNc DA neurons are two major pathological hallmarks in PD. The subsequent dopamine depletion in the striatum and other nuclei in the basal ganglia forms the putative pathophysiological process underlying the motor and non-motor symptoms of PD [2,7,8]. Dopamine compensation is the major therapeutic strategy for PD but is less effective for pain than for motor symptoms [2,7,9]. These studies suggest that pathological processes other than dopamine depletion may be involved in motor symptoms and pain in PD.

Accumulating evidence implicates astrocytes in PD pathology [10–12]. Reactive astrocytes are abundant in the striatum and substantia nigra in PD patients and animal models [13,14]. These reactive astrocytes release proinflammatory and neurotoxic molecules that cause accumulation of α-synuclein, leading to neuronal and synaptic damage [15]. On the other hand, reactive astrocytes also secrete glial-derived neurotrophic factor (GDNF), which promotes neuronal survival, growth of axons and dendrites, and formation of synapses [16] and can attenuate damage to the nigrostriatal DA system from neurotoxins [17]. Inflammatory and neuroprotective astrocytes possess distinct gene expression profiles and are classified as A1 and A2 astrocytes, respectively [14,18]. Activation and proliferation of microglia are commonly seen in degenerative diseases, including PD [19]. As with astrocytes, reactive microglia are also divided into inflammatory M1 microglia and neuroprotective M2 microglia [19,20]. M1 microglia release interleukin 1 alpha (IL-1α),

* Corresponding authors.
E-mail addresses: xchengxj@xzhmu.edu.cn (C. Xiao), chunyi.zhou@xzhmu.edu.cn (C. Zhou).

https://doi.org/10.1016/j.fmre.2023.05.020

tumor necrosis factor alpha (TNF-α), and the complement component C1q, which activate A1 astrocytes to exacerbate neuronal damage, and A1 astrocytes release α-synuclein to activate M1 microglia [14,21,22]. Therefore, interactions between microglia and astrocytes may affect the development of PD. However, the role of striatal microglia and astrocytes in pain and motor symptoms in PD has not been well studied.

Pathological studies have shown that loss of DA terminals in the striatum precedes DA neuronal death in the SNc [23,24]. This suggests that the degeneration of the nigrostriatal DA system may be initiated at striatal DA terminals. Furthermore, intraventricular injection of 6-OHDA leads to astrogliosis in the striatum [10]. Thus, reactive astrocytes in the striatum may play an important role in the early stages of PD. In the present study, we established a hemiparkinsonian mouse model of PD via unilateral injection of 6-hydroxydopamine (6-OHDA) and observed subsequent activation and polarization of microglia and astrocytes in the dorsal striatum, as well as astrocyte dysfunction. Blockade of microglia activation reduced the polarization of microglia and astrocytes to the inflammatory (M1, A1) phenotypes in the dorsal striatum, attenuated the damage to the nigrostriatal DA system, and mitigated mechanical allodynia and motor deficits in parkinsonian mice. This study provides a link between M1 microglia and A1 astrocytes in the dorsal striatum and hyperalgesia in an early-stage parkinsonian mouse model.

2. Materials and methods

2.1. Animals

The care and use of animals and the experimental protocols used in this study were approved by the Institutional Animal Care and Use Committee and the Office of Laboratory Animal Resources of Xuzhou Medical University under the Regulations for the Administration of Affairs Concerning Experimental Animals (1988) in China. Male C57/BL6 wild-type mice (5–7 months old) were group housed ($\leq$ 4) in a standard 12 h light/dark cycle with free access to food and water. All behavioral experiments were performed during the light cycle. Efforts were made to minimize animal suffering and to reduce the number of mice used.

2.2. Unilateral 6-hydroxydopamine (6-OHDA) lesion of SNc DA neurons and minocycline injections

The hemiparkinsonian mouse model was established according to the protocol described previously with slight modifications [8,25,26]. In brief, mice were intraperitoneally (i.p.) injected with desipramine (20 mg/kg) 30 min prior to surgery to protect noradrenergic neurons and were then deeply anesthetized with sodium pentobarbital. A small craniotomy was made above the right medial forebrain bundle (MFB). The coordinates for the MFB were 0.5 mm rostral to bregma, 1.2 mm lateral to the midline, and 4.8 mm deep relative to bregma. 0.3 μl 6-OHDA (12 μg/μl in 0.2% ascorbic acid/normal saline) was stereotaxically injected at a rate of 0.1 μl/min with a microinjector (KD Scientific, Holliston, MA, USA). Control mice were injected with 0.3 μl normal saline containing 0.2% ascorbic acid. Post-surgery care was carried out similarly for both control and 6-OHDA-injected mice. The parkinsonian model was confirmed by the loss of dopaminergic neurons in the SNc and dopaminergic fibers in the dorsal striatum, bradykinesia, and apomorphine-induced contralateral rotations [8,25,27].

In some parkinsonian mice, immediately after 6-OHDA injection, a guide cannula was implanted above the right dorsal striatum (0.3 mm caudal to bregma, 2 mm lateral to the midline, 3 mm in depth from bregma, 0.5 mm above the planned injection site) and fixed to the skull with dental cement. Minocycline (10 μg/μl, 200 nl) or 200 nl saline was injected into the dorsal striatum through a needle (0.5 mm longer than the guide cannula) inserted into the guide cannula at a rate of 80 nl/min with a microinjector (KD Scientific, Holliston, MA, USA). Minocycline injections were performed once per day for 7 days starting on the first day after 6-OHDA injection.

2.3. Quantitative real-time polymerase chain reaction (qRT-PCR)

2.3.1. RNA extraction and cDNA synthesis

Mice were euthanized in a CO_2 chamber and decapitated with a guillotine. The brains were removed, washed with ice-cold artificial cerebrospinal fluid (ACSF), placed in a mouse brain module with coronal slots 0.5 mm apart on both sides, and cut into 2.5 mm thick sections. The dorsal striatum was dissected from the section, placed and sealed in a nuclease-free tube, and frozen in liquid nitrogen. Total RNA was extracted from the striatum using TRIzol reagent (Invitrogen, Carlsbad, CA). 2 μg of each RNA sample was reverse-transcribed into cDNA using a PrimeScript cDNA synthesis kit (TaKaRa PrimeScript RT reagent Kit, Takara Biomedical Co. Ltd, Kusatsu, Japan) according to supplier's protocol. Briefly, the RNA sample was mixed with PrimeScript RT Master Mix and RNase-free water, incubated at 37 °C for 15 min, at 85 °C for 5 s, and then held at 4 °C. Reaction products were diluted 5 × in RNAase-free ddH_2O and kept at 4 °C or −80 °C until used in the experiments.

2.3.2. Standard qRT-PCR

Quantitative RT-PCR (qPCR) was run using 1.5 μl cDNA and a SYBR green qPCR master mix (Servicebio, Wuhan, China) according to the supplier's protocol. The cycling program was 5 min at 95 °C followed by 40 cycles of 95 °C for 15 s, 60 °C for 30 s, and 72 °C for 30 s in an ABI QuatStudio7 Flex (Life Technologies, Carlsbad, CA). After completion of the qPCR, a melting curve of amplified products was determined. Each sample was amplified in two duplicated tubes. The relative expression level for each gene was calculated using the $2^{-\Delta\Delta Ct}$ method, and all PCR values were normalized with the house-keeping gene GAPDH. Primer sequences for mice are listed in Table 1.

2.4. Brain-slice preparation and patch-clamp recordings

We sectioned mouse brains coronally using protocols reported previously with minor modifications [28,29]. In brief, mice were euthanized with CO_2 and quickly subjected to cardiac perfusion with ice-cold modified sucrose-based artificial cerebral spinal fluid (sACSF). The brain

Table 1
Primer sequence for genes measured in qPCR analysis.

gene	Forward primer	Reverse primer
Iba-1	GGATTTGCAGGGAGGAAAAG	TGGGATCATCGAGGAATTG
Cd68	TGGGATCATCGAGGAATTG	ATTTGAATTTGGGCTTGGAG
Il-1β	TTCAGGCAGGCAGTATCACTC	GAAGGTCCACGGGAAAGACAC
Tnf-α	CCCTCACACTCAGATCATCTTCT	GCTACGACGTGGGCTACAG
Cd86	GAGCGGGATAGTAACGCTGA	GGCTCTCACTGCCTTCACTC
iNos	CAGCTGGGCTGTACAAACCTT	CATTGGAAGTGAAGCGTTTCG
Cd206	CTTCGGGCCTTTGGAATAAT	TAGAAGAGCCCTTGGGTTGA
Tgf-β	CAGAGCTGCGCTTGCAGAG	GTCAGCAGCCGGTTACCAAG
Il-10	AAGCTCCAAGACCAAGGTGTC	AGGAAGAACCCCTCCCATCA
Ym-1	GGGCATACCTTTATCCTGAG	CCACTGAAGTCATCCATGTC
Arg-1	CTTGGCTTGCTTCGGAACTC	GGAGAAGGCGTTTGCTTAGTTC
Gapdh	AGGTCGGTGTGAACGGATTTG	TGTAGACCATGTAGTTGAGGTCA
Gfap	AGAAAGGTTGAATCGCTGGA	CGGCGATAGTCGTTAGCTTC
Hspb1	GACATGAGCAGTCGGATTGA	GGATGGGGTGTAGGGGTACT
Osmr	GTGAAGGACCCAAAGCATGT	GCCTAATACCTGGTGCGTGT
Steap4	CCCGAATCGTGTCTTTCCTA	GGCCTGAGTAATGGTTGCAT
Lcn2	CCACCACGGACTACAACCAG	TCCTTGGTTCTTCCATACAGGG
Ggta1	GTGAACAGCATGAGGGGTTT	GTTTTGTTGCCTCTGGGTGT
H2-D1	TCCGAGATTGTAAAGCGTGAAGA	ACAGGGCAGTGCAGGGATAG
H2-T23	GGACCGCGAATGACATAGC	GCACCTCAGGGTGACTTCAT
Ligp1	GGGGCAATAGCTCATTGGTA	ACCTCGAAGACATCCCCTTT
Serping1	ACAGCCCCCTCTGAATTCTT	GGATGCTCTCCAAGTTGCTC
Cd109	CACAGTCGGGAGCCCTAAAG	GCAGCGATTTCGATGTCCAC
Sphk1	GATGCATGAGGTGGTGAATG	TGCTCGTACCCAGCATAGTG
Tm4sf1	GCCCAAGCATATTGTGGAGT	AGGGTAGGATGTGGCACAAG
S1pr3	AAGCCTAGCGGGAGAGAAAC	TCAGGGAACAATTGGGAGAG
B3gnt5	CGTGGGGCAATGAGAACTAT	CCCAGCTGAACTGAAGAAGG
C1q	TCACCAACCAGGAGAGTCCA	CACCTGAAAGAGCCCCTTGT
Il-1α	GCACCTTACACCTACCAGAGT	AAACTTCTGCCTGACGAGCTT

was removed and sliced into 300-μm-thick slices with a Leica VT-1200S vibratome (Nussloch, Germany) in ice-cold modified sACSF, saturated with 95% O_2/5% CO_2, containing (mM): 85 NaCl, 70 sucrose, 25 glucose, 24 $NaHCO_3$, 4 $MgCl_2$, 2.5 KCl, 1.2 NaH_2PO_4, and 0.5 $CaCl_2$. Brain slices containing the striatum were recovered at 32 ˚C for 1 h in a holding chamber filled with carbogenated sACSF. Sixty min later, the holding chamber with brain slices was transferred to regular ACSF (25 ˚C, carbogenated, containing 125 NaCl, 26 $NaHCO_3$, 11 glucose, 2.5 KCl, 2.4 $CaCl_2$, 1.2 NaH_2PO_4 and 1.2 $MgCl_2$) for patch-clamp recordings and live imaging.

Striatal slices were stained with a red fluorescent astrocyte marker, sulforhodamine 101 (SR-101, 5 μM) in carbogenated ACSF for 35 min at 34 ˚C [29] and were subsequently returned to dye-free ACSF for at least 30 min before patch-clamp recordings. SR-101-labeled astrocytes were identified using near-infrared DIC and fluorescent illumination under an upright FN-1 Nikon microscope equipped with a CCD camera (Flash 4.0 LTE, Hamamatsu, Japan) and a 40 × water-immersion objective (WD, 3.5 mm; NA, 0.80). Patch electrodes had a resistance of 11–13 MΩ when filled with an intrapipette solution with pH 7.2 and osmolarity 300 mOsm/L (in mM: 135 K gluconate, 10 HEPES, 5 KCl, 2 Mg-ATP, 0.5 $CaCl_2$, 0.2 EGTA and 0.1 GTP). Electrophysiological signals were recorded with a MultiClamp 700B amplifier, a Digidata 1552B analog-to-digital converter, and pClamp 10.7 software (Molecular Devices, San Jose, CA). Data were sampled at 10 kHz and low-pass filtered at 2 kHz.

The junction potential between the patch pipette and the bath solution was nulled just before gigaseal formation. Series resistance was monitored without compensation throughout the experiment, and the data were discarded if the series resistance (15–20 MΩ) changed by > 20% during whole-cell recordings.

2.5. Immunohistochemistry

Mice were sacrificed in a CO_2 chamber and subjected to transcardiac perfusion with phosphate-buffered saline (PBS) followed by 4% paraformaldehyde (PFA). Brains were removed and post-fixed in 4% PFA for 4–6 h followed by gradient sucrose dehydration for two days at 4 ˚C. After dehydration, brains were sectioned into 30 μm sections with a Leica cryostat (CM1950, Nussloch, Germany), and the sections were mounted onto glass slides and kept at −20 ˚C.

The mounted frozen sections were washed twice (10 min each) with cold PBS, blocked for 1 h at room temperature in 0.1% Triton X-100 and 5% donkey serum in PBS, followed by incubation in primary antibodies (1: 500, chicken anti-TH, Aves Lab; 1: 500 rabbit anti-Iba-1, Wako; 1: 500 mouse anti-GFAP, Santa Cruz) in 0.1% Triton X-100 and 1% donkey serum in PBS at 4 ˚C for 24 h. After three times (10 min each) washes with PBS, the slices were incubated with secondary antibody (1:500, donkey anti-chicken, donkey anti-rabbit, donkey anti-mouse, Jackson ImmunoResearch) in PBS at room temperature for 2 h. The sections were washed three times (10 min each) with PBS, dried at room temperature, and cover-slipped in mounting medium.

The stained slices were imaged under 20 × and 60 × (oil) objectives with a Zeiss LSM 880 confocal microscope (Zeiss, Wetzlar, Germany). The images were processed with Image J (NIH, Bethesda, MD).

2.6. Behavioral tests

Open-field test Mice were allowed to habituate in a testing room for at least 2 h. Then, motor behaviors in an open-field area (30 cm in diameter) were recorded with a video camera controlled by Ethovision XT 14 software (Noldus Information Technology, Wageningen, Netherland).

von Frey filament test Mechanical pain thresholds were measured in acclimated mice via the up–down method using von Frey filaments [30]. In brief, the first von Frey filament (0.41 g) was applied to the plantar surface of the hind paw. If a withdrawal response was observed within 2 s, the next lower force filament was used. Conversely, if the filament failed to elicit a withdrawal response, the next filament with higher force was applied. After the first withdrawal response occurred, this paradigm continued until a total of six responses, starting from the one before the first withdrawal response, were recorded. A score ranging between 0.01 and 3.0 g was assigned in the case of four consecutive positive responses to filaments with decreasing force, or three consecutive negative responses to filaments with increasing force. A 50% paw withdrawal threshold (PWT) was determined using these responses, as described previously [30].

In all the above experiments, the investigators were blind to the identity of the mice.

2.7. Chemicals

DL-2-Amino-5-phosphonovaleric acid lithium salt (APV), ascorbic acid, and 6-cyano-7-nitro-quinoxaline-2, 3-dione disodium salt hydrate (CNQX) were purchased from Tocris (Park Ellisville, MO). 6-hydroxydopamine (6-OHDA), barium chloride, and desipramine were purchased from Sigma Aldrich (St. Louis, MO). Biocytin was purchased from Vector laboratories (Newark, CA). Minocycline (MC) was purchased from MedChemExpress (Monmouth Junction, NJ). Sulforhodamine 101 (SR-101) was purchased from Thermo Fisher Scientific (Waltham, MA).

2.8. Data analysis

All statistical analyses were performed in GraphPad Prism 7.0. Summary data are presented as scatter plots and bar charts. We used a two-tailed paired *t*-test, one-way ANOVA, two-way ANOVA, or the Kruskal–Wallis one-way ANOVA to analyze the data, as indicated in the Results, depending on whether the data passed tests of normality and equal variance. Values of $P < 0.05$ were considered statistically significant.

3. Results

3.1. Hemiparkinsonian mice established by 6-OHDA-lesion of the nigrostriatal dopaminergic system show bradykinesia and pain-like behavior

To establish a unilateral parkinsonian mouse model, we intracranially injected 6-OHDA into the medial forebrain bundle (MFB) in the right hemisphere of mice and examined time-dependent damage to the nigrostriatal dopaminergic (DA) system and time-dependent alterations in motor and pain-like behaviors (Fig. S1a). We observed that this procedure caused a dramatic reduction in TH-positive neurons in the SNc (Fig. S1b,c) and in TH immunoreactivity in the dorsal striatum (Fig. S1d,e) on the 6-OHDA injection side. These results indicate that 6-OHDA lesioned the ipsilateral nigrostriatal DA system. Two-way ANOVA analysis revealed that 6-OHDA injection led to a time-dependent lesion of striatal DA axonal fibers that was much faster and more robust than the lesion of SNc DA neurons (Fig. S1c,e) (Time: $F_{(3, 18)} = 35.18$, $P < 0.0001$; SNc vs Striatum: $F_{(1, 6)} = 48.48$, $P = 0.0004$, $n = 5$ at each time point in each area, two-way ANOVA). Therefore, damage to the DA system in both the striatum and the SNc may be important to the pathophysiology that underlies parkinsonian symptoms.

In addition to the damage in the nigrostriatal DA system, we observed motor deficits (bradykinesia and apomorphine-induced contralateral rotations) (Fig. S1f,g) and bilateral mechanical allodynia in 6-OHDA-lesioned mice (Fig. S1h,i).

These data indicate that we successfully established a parkinsonian mouse model exhibiting both motor deficits and mechanical allodynia.

3.2. Microglia in the dorsal striatum are modified in parkinsonian mice

To examine whether microglia are modified in the dorsal striatum in parkinsonian mice, we injected 6-OHDA into the right MFB and tested the activation and differentiation of microglia in the dorsal striatum 3,

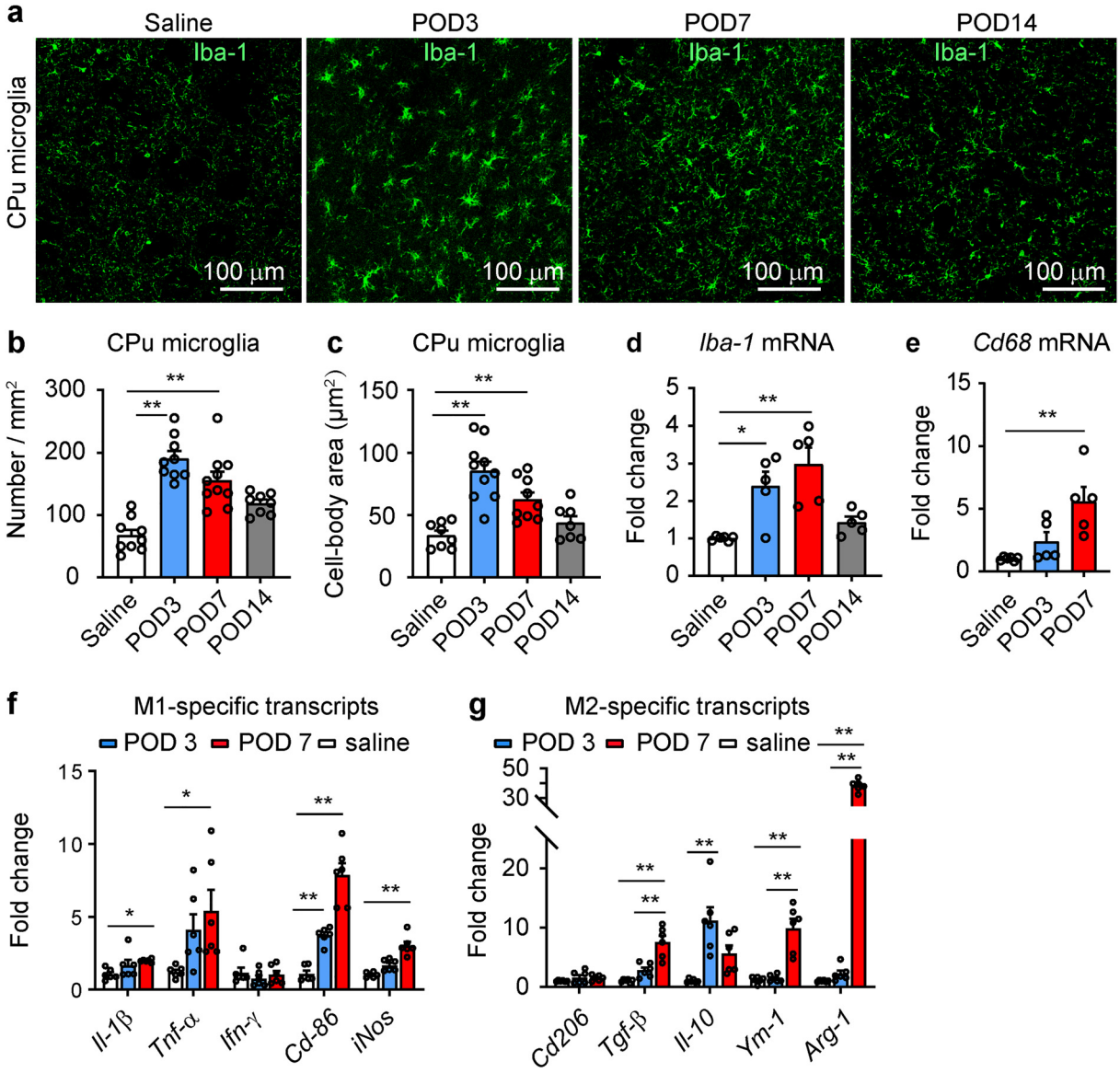

Fig. 1. Microglia in the striatum are modified in parkinsonian mice. (a) Representative images showing activation of microglia in the ipsilateral dorsal striatum 3, 7, and 14 days after unilateral 6-OHDA injection into the medial forebrain bundle. Green represents Iba-1-positive microglia. (b) Number of Iba-1-positive microglia in the striatum 3 ($n = 9$), 7 ($n = 10$), and 14 ($n = 8$) days after 6-OHDA injection. $F_{(3, 32)} = 23.61$, $P < 0.0001$. (c) Area of Iba-1-positive microglia in the striatum 3, 7, and 14 days after 6-OHDA injection. $F_{(3, 30)} = 15.44$, $P < 0.0001$. (d) Level of *Iba-1* mRNA in the striatum 3, 7, and 14 days after 6-OHDA injection, relative to the average in saline mice. $F_{(3, 17)} = 10.22$, $P = 0.0004$. (e) Level of *Cd68* mRNA in the striatum 3, 7, and 14 days after 6-OHDA injection, relative to the average in saline mice. $F_{(2, 13)} = 9.85$, $P = 0.0025$. (f) mRNA level of M1-microglia-specific genes in the striatum 3, 7, and 14 days after 6-OHDA injection, relative to the average in saline mice. *Il-1β*: $F_{(2, 15)} = 3.99$, $P = 0.04$. *Tnf-α*: $F_{(2, 15)} = 4.20$, $P = 0.036$. *Ifn-γ*: $F_{(2, 15)} = 0.54$, $P = 0.60$. *Cd86*: $F_{(2, 15)} = 46.5$, $P < 0.0001$. *iNos*: $F_{(2, 15)} = 29.35$, $P < 0.0001$. $n = 6$ in each group. (g) mRNA level of M2-microglia-specific genes in the striatum 3, 7, and 14 days after 6-OHDA injection, relative to the average in saline mice. *Cd206*: $F_{(2, 15)} = 1.49$, $P = 0.26$. *Tgf-β*: $F_{(2, 15)} = 25.55$, $P < 0.0001$. *Il-10*: $F_{(2, 15)} = 10.51$, $P = 0.001$. *Ym-1*: $F_{(2, 15)} = 28.39$, $P < 0.0001$. *Arg-1*: $F_{(2, 15)} = 494.10$, $P < 0.0001$. $n = 6$ in each group. One-way ANOVAs with Bonferroni tests were used for (b-g). * $P < 0.05$; ** $P < 0.01$. n.s, not significant.

7, and 14 days after 6-OHDA injection. After immunostaining of striatal sections with an Iba-1 antibody to label activated microglia, we observed a time-dependent alteration in striatal microglia after 6-OHDA injection into the MFB. Both the number and cell-body size of striatal microglia were significantly increased 3 and 7 days after 6-OHDA injection (Fig. 1a-c). These results were confirmed by an increase in *Iba-1* and *Cd68* mRNA at the same time points (Fig. 1d,e). The changes in microglia morphology and microglia markers *Iba-1* and *Cd68* were diminished by day 14 after 6-OHDA injection. These data suggest that microglia activation occurs at the early stages in hemiparkinsonian mice.

Activated microglia are heterogeneous and are generally classified as inflammatory M1 microglia or neuroprotective M2 microglia according to their effects on neurons [19,20]. Each type expresses specific genes [19,20]. Therefore, the upregulation of specific genes can indicate the polarization of microglia into the M1 or M2 phenotype. As illustrated in Fig. 1f, M1 microglia-specific genes, including *Il-1β, Tnf-α, Ifn-γ, Cd86*, and *iNos*, were significantly upregulated in the dorsal striatum 3 and 7 days after 6-OHDA injection, following the same trend as *Iba-1* and *Cd68* (Fig. 1d,e). Most M2-specific genes, such as *Cd206, Tgf-β, Il-10, Ym-1*, and *Arg-1*, were upregulated in the dorsal striatum 7 days after 6-OHDA injection (Fig. 1g).

These results suggest that 6-OHDA lesion induces activation of microglia with both the M1 and M2 phenotypes, with an earlier enhancement of polarization to M1 microglia than to M2 microglia.

3.3. Astrocytes in the dorsal striatum are modified in parkinsonian mice

Activated M1 microglia release IL-1β and TNF-α, which may activate astrocytes [14,21]. We next examined whether striatal astrocytes were modified by 6-OHDA injection. Our immunohistochemistry data show that GFAP-labeled reactive astrocytes were increased 3–14 days after 6-OHDA injection (Fig. 2a,b). Note that the peak increase occurred 7 days after 6-OHDA injection (Fig. 2b). Reactive astrocytes can enhance coupling with each other through gap junctions [31]. To test whether 6-OHDA-activated striatal astrocytes have enhanced coupling, we performed patch-clamp recordings from astrocytes. Before recordings, we incubated live brain slices with an astrocyte-specific red fluorescent dye, SR-101, to label astrocytes and added a gap-junction-permeable molecule, biocytin, into the pipette solution. Thus, biocytin labels individual recorded astrocytes and other astrocytes connected to them via gap junctions. This procedure allowed us to measure the coupling among astrocytes. After recording from SR-101-labeled astrocytes and post-hoc staining of biocytin with Alexa 488-conjugated streptavidin, we observed that biocytin labeled more striatal astrocytes in parkinsonian mice than control mice. This suggests that lesioning with 6-OHDA enhances coupling among astrocytes (Fig. 2c,d). Besides being activated, astrocytes had enlarged cell bodies, with the largest size occurring 7 days after 6-OHDA injection (Fig. 2e). Our qRT-PCR data show that GFAP mRNA increased about 20-fold 3 and 7 days after 6-OHDA injection, but dramatically recovered 14 days after 6-OHDA injection (Fig. 2f). Increases in mRNA were also observed for other genes associated with reactive astrocytes (pan-reactive astrocyte genes), including *Osmr, S1pr3*, and *Lcn2*, 3 and 7 days after 6-OHDA injection (Fig. 2g). Therefore, 6-OHDA injection in the MFB causes activation of striatal astrocytes.

Reactive astrocytes consist of inflammatory A1 astrocytes and protective A2 astrocytes [21,32]. We next examined the mRNA levels of genes specifically expressed in A1 or A2 astrocytes. We found that A1-specific genes (*Ggta1, H2-D1, H2T-23, Ligp1*, and *Serping1*) (Fig. 2h) and A2 -specific genes (*Cd109, Sphk1*, and *B3gnt5*) (Fig. 2i) were upregulated in the striatum 3 and 7 days after 6-OHDA injection. Although the time to reach the highest upregulation differed among these genes, our data suggest that 6-OHDA injection enhanced polarization of astrocytes into both A1 and A2 types. Indeed, 6-OHDA injection increased mRNA of *C1q, Il-1α*, and *Tnf-α* (Fig. 2j-l), which are important for the interaction between M1 microglia and A1 astrocytes [14].

These results show that following activation of microglia, astrocytes proliferate and are polarized into both A1 and A2 astrocytes.

3.4. Electrophysiological properties of striatal astrocytes are modified in parkinsonian mice

We next examined the electrophysiological properties of striatal astrocytes. In this set of experiments, we used SR-101 to label astrocytes in live brain slices and then performed whole-cell patch-clamp recordings to evaluate the function of voltage-gated ion channels in astrocytes (Fig. 3a). In SR-101-labeled astrocytes in the dorsal striatum, we observed that the voltage steps evoked larger currents in striatal astrocytes from 6-OHDA mice than from control mice (Fig. 3b-d). As the responses to voltage steps are mainly mediated by voltage-gated potassium channels (Kvs), these data suggest that the function of these channels is enhanced in 6-OHDA mice. We observed that striatal astrocytes in 6-OHDA mice exhibited more hyperpolarized resting membrane potentials (Fig. 3e), higher membrane conductance (Fig. 3f), and larger membrane capacitance (Fig. 3g) than those in control mice. These biophysical alterations are consistent with enhancement of Kvs and enlargement of cell bodies in striatal astrocytes in 6-OHDA mice. We next calculated current density by dividing the voltage- induced currents by the capacitance of the astrocytes. The I-V curves of striatal astrocytes from control and 6-OHDA mice almost overlapped (Fig. 3h). Therefore, the enhancement of Kvs properties may be related to the enlargement of the astrocytes rather than an increase in channel density.

Astrocytes are implicated in the homeostasis of extracellular potassium and glutamate concentrations, which are critical for the maintenance of neuronal physiological function in the central nervous system [33]. The inwardly rectifying potassium channel 4.1 ($Kir_{4.1}$) and glutamate transporters in the astrocytes are important components for this [34]. Therefore, we next examined the effect of 6-OHDA treatment on the function of $Kir_{4.1}$ channels and glutamate transporters.

To isolate $Kir_{4.1}$ currents, we recorded the membrane currents evoked by voltage steps before and during perfusion of 100 μM $BaCl_2$ and subtracted the currents in the presence of Ba^{2+} from those in the absence of Ba^{2+} [34] (Fig. 4a). We observed that Ba^{2+}-sensitive $Kir_{4.1}$ currents were reduced in striatal astrocytes in 6-OHDA mice relative to those in control mice (Fig. 4b).

Glutamate-evoked responses in astrocytes are mediated by glutamate receptors and glutamate transporters [35]. To understand whether 6-OHDA affects the ability of astrocytes to cope with elevated extracellular glutamate, we puffed 100 μM glutamate onto voltage-clamped astrocytes (at a holding potential of −80 mV) and included 20 μM CNQX and 50 μM APV in the perfusate to block ionotropic glutamate receptors (Fig. 4c). Under these conditions, glutamate-induced responses in the astrocytes should be mainly mediated by glutamate transporters [35]. We observed that glutamate-transporter-mediated responses recorded from striatal astrocytes in 6-OHDA mice were significantly smaller than those recorded from control mice (Fig. 4d,e).

Therefore, 6-OHDA treatment not only changed the biophysical properties of astrocytes, but also impaired the function of $Kir_{4.1}$ channels and glutamate transporters. These effects may disrupt normal potassium and glutamate homeostasis in the striatum.

3.5. Minocycline normalizes microglial changes in parkinsonian mice

Minocycline inhibits the activation and polarization of microglia [36] and exhibits anti-inflammatory and neuroprotective effects in many neurological diseases [37,38]. We wondered whether it would mitigate inflammation in the striatum in parkinsonian mice. To answer this question, we administered minocycline intraperitoneally (i.p.) once per day after 6-OHDA injection in the MFB until the mice were sacrificed 3 or 7 days later. As illustrated in Fig. 5a-e, minocycline significantly attenuated microglia activation 7 days after 6-OHDA injection: minocycline reduced the 6-OHDA-induced increase in the number and cell body size of Iba-1-positive microglia without affecting the morphological arborization in these microglia. We then analyzed the effects of minocycline on gene expression in microglia 3 and 7 days after 6-OHDA injection. Three days after 6-OHDA injection, the expression of most genes in reactive microglia (Fig. 5f,g) and those specific to M1 and M2 microglia (Fig. 5h,i) were not dramatically enhanced, either with or without minocycline administration. Seven days after 6-OHDA injection, the expression of most genes in reactive microglia (Fig. 5j,k) and those specific to M1 and M2 microglia (Fig. 5l,m) were dramatically upregulated. Interestingly, minocycline attenuated the 6-OHDA-induced increase of most M1-specific genes (Fig. 5l), but not M2-specific genes (Fig. 5m). These results suggest that minocycline mitigates 6-OHDA-induced activation of microglia, particularly the M1 phenotype.

3.6. Minocycline attenuates activation of astrocytes in parkinsonian mice

As shown in Fig. 5, minocycline effectively inhibited 6-OHDA-induced activation of M1 microglia. If the activation of astrocytes depends on activation of M1 microglia in parkinsonian mice, minocycline may mitigate the 6-OHDA-induced activation of A1 astrocytes. To test this postulation, we examined the effect of i.p. injection of minocycline on astrocyte activation in the striatum in parkinsonian mice. Similar to microglia activation in 6-OHDA mice, astrocyte activation and polarization was partially reversed by minocycline administration

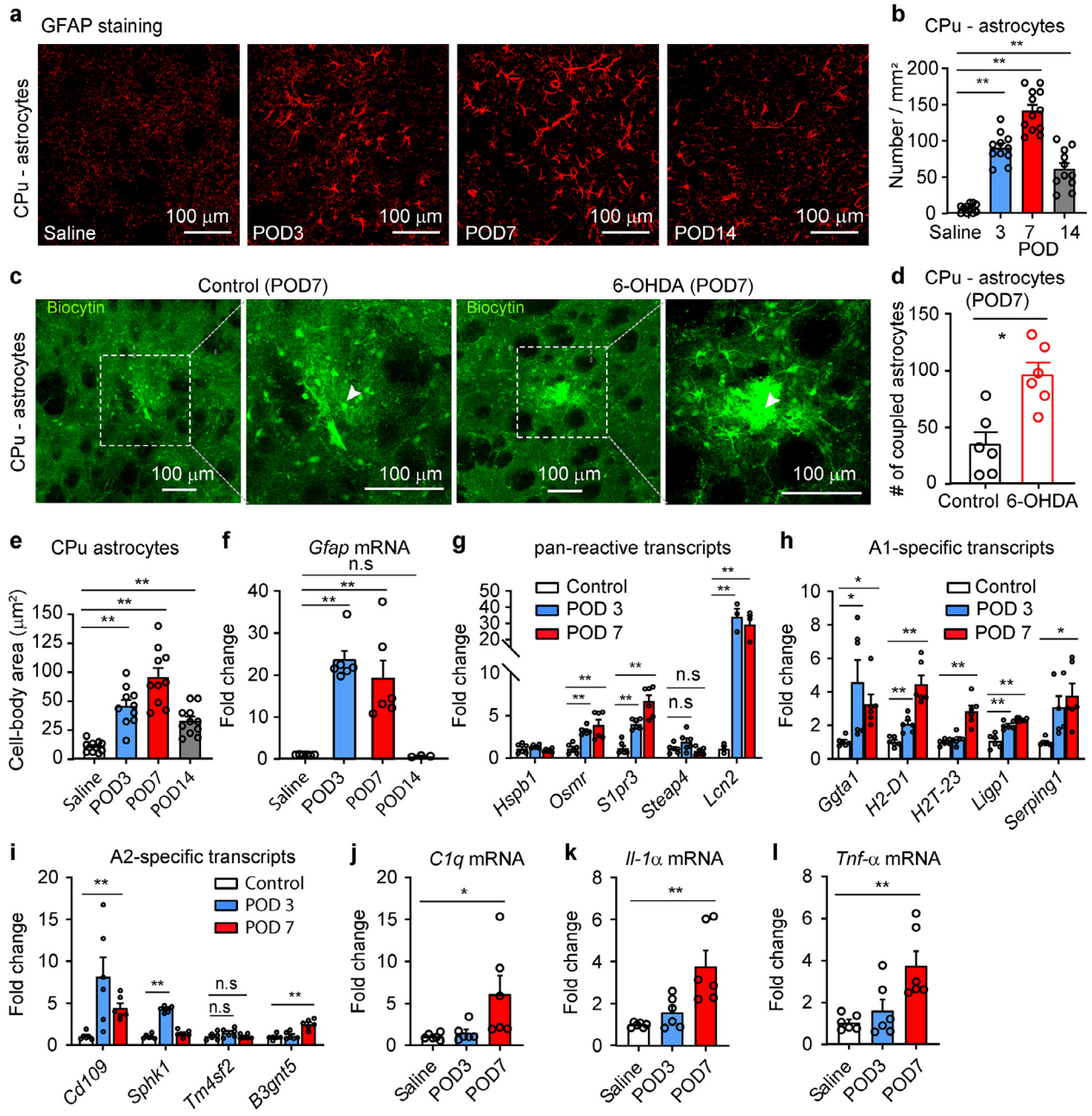

Fig. 2. Astrocytes in the striatum are modified in parkinsonian mice. (a) Representative images showing activation of astrocytes in the ipsilateral dorsal striatum 3, 7, and 14 days after unilateral 6-OHDA injection into the medial forebrain bundle. Red represents GFAP-positive astrocytes. (b) Number of GFAP-positive astrocytes in the striatum 3, 7, and 14 days after 6-OHDA injection. $F_{(3, 41)} = 72.75$, $P < 0.0001$. (c-d) Representative images and summary showing astrocytes labeled with biocytin (green) during patch-clamping in live striatal slices from control ($n = 11$) and 6-OHDA ($n = 13$) mice. $t = 3.93$, $P = 0.003$. (e) Area of GFAP-positive astrocytes in the striatum 3, 7, and 14 days after 6-OHDA injection. $F_{(3, 38)} = 25.97$, $P < 0.0001$. (f) Level of *Gfap* mRNA in the striatum 3, 7, and 14 days after 6-OHDA injection, relative to the average in control mice. $F_{(3, 17)} = 17.38$, $P < 0.0001$. (g) mRNA level of genes commonly expressed in reactive astrocytes (pan-reactive genes) in the striatum 3 and 7 days after 6-OHDA injection, relative to the average in control mice. Pan-reactive transcripts: *Hspb1*, $F_{(2, 15)} = 2.31$, $P = 0.13$; *Osmr*, $F_{(2, 15)} = 11.91$, $P = 0.0008$; *S1pr3*, $F_{(2, 15)} = 33.70$, $P < 0.0001$; *Steap4*, $F_{(2, 15)} = 3.63$, $P = 0.05$; *Lcn2*, $F_{(2, 15)} = 17.08$, $P = 0.003$; $n = 6$ in each group. (h) mRNA level of A1-astrocyte-specific genes in the striatum 3 and 7 days after 6-OHDA injection, relative to the average in control mice. A1 transcripts: *Ggta1*, $F_{(2, 15)} = 4.64$, $P = 0.03$; *H2-D1*, $F_{(2, 15)} = 28.57$, $P < 0.0001$; *H2T-23*, $F_{(2, 15)} = 22.37$, $P < 0.0001$; *Ligp1*, $F_{(2, 15)} = 25.61$, $P < 0.0001$; *Serping1*, $F_{(2, 15)} = 6.27$, $P = 0.01$; $n = 6$ in each group. (i) mRNA level of A2-astrocyte-specific genes in the striatum 3 and 7 days after 6-OHDA injection, relative to the average in control mice. A2 transcripts: *Cd109*, $F_{(2, 15)} = 6.41$, $P = 0.01$; *Sphk1*, $F_{(2, 15)} = 159.7$, $P < 0.0001$; *Tm4sf1*, $F_{(2, 15)} = 1.84$, $P = 0.19$; *B3gnt5*: $F_{(2, 15)} = 20.85$, $P < 0.0001$; $n = 6$ in each group. (j-l) mRNAs level of *C1q*, *Il-1α*, and *Tnf-α* in the striatum 3 and 7 days after 6-OHDA injection, relative to the average in control mice. $n = 6$ in each group. (j) *C1q*: $F_{(2, 15)} = 4.66$, $P = 0.03$. (k) *Il-1α*: $F_{(2, 15)} = 10$, $P = 0.002$. (l) *Tnf-α*: $F_{(2, 15)} = 7.90$, $P = 0.004$. A two-tailed *t*-test was used for (d). One-way ANOVAs with Bonferroni tests were used for (b) and (e-l). * $P < 0.05$; ** $P < 0.01$. n.s, not significant.

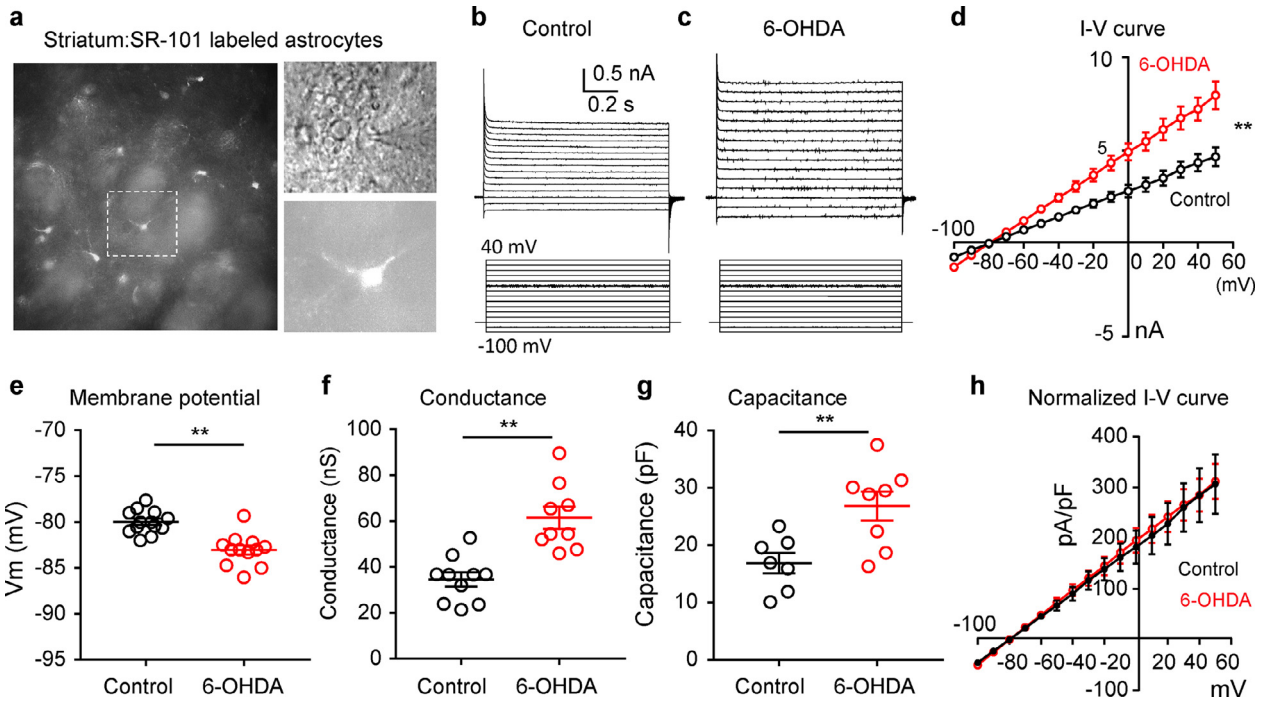

Fig. 3. Electrophysiological properties of astrocytes in the striatum are impaired in parkinsonian mice. (a) Left panel, a representative image showing SR-101-labeled astrocytes in the striatum (left panel). Upper right panel, a bright-field image showing a voltage-clamped astrocyte. Lower right panel, an SR-101-positive astrocyte recorded in voltage-clamp mode. (b-c) Representative traces (upper panel) showing the responses to voltage steps (lower panel) in an astrocyte from a control mouse and an astrocyte from a 6-OHDA mouse. (d) I-V curves in astrocytes from control (n = 13) and 6-OHDA (n = 12) mice. Group: $F_{(1, 208)}$ = 122.50, P < 0.0001. Voltage: $F_{(15, 208)}$ = 83.60, P < 0.0001. (e-g) Membrane potential, conductance, and capacitance of SR-101-labeled striatal astrocytes in control and 6-OHDA mice. (e) t = 5.18, P < 0.0001, n = 13 in control, n = 12 in 6-OHDA. (f) t = 4.76, P = 0.0002, n = 10 in control, n = 9 in 6-OHDA. (g) t = 3.15, P = 0.008, n = 7 in control, n = 8 in 6-OHDA. (h) Density of voltage-step-induced currents in striatal astrocytes from control and 6-OHDA-lesioned mice. Group: $F_{(1, 208)}$ = 0.32, P = 0.57. Voltage: $F_{(15, 208)}$ = 40.12, P < 0.0001. Two-way ANOVAs were used for (d,h). Two-tailed t-tests were used for (e-g). ** P < 0.01. n.s, not significant.

(Fig. 6). Specifically, minocycline significantly reduced the number of GFAP-positive astrocytes in the striatum in 6-OHDA mice (Fig. 6a,b), but did not change the arborization of astrocytes (Fig. 6d,e). In contrast to striatal microglia, striatal astrocytes in 6-OHDA-lesioned mice did not show a reduction in cell-body size after minocycline administration (Fig. 6c). Three days after 6-OHDA injection, minocycline did not change the expression of *Gfap, C1q*, or *Il-1α*, pan-reactive genes, or those specific to A1 or A2 astrocytes (Fig. 6f-k). Seven days after 6-OHDA lesion, the transcription of *Gfap, C1q*, and *Il-1α*, pan-reactive genes (Fig. 6l-o), and some genes specific to A1 and A2 astrocytes (Fig. 6p,q) were dramatically upregulated. The upregulation of pan-reactive and A1-specific genes, but not A2-specific genes, was significantly attenuated by minocycline treatment. These results suggest that minocycline mitigates 6-OHDA-induced activation of astrocytes, particularly A1 astrocytes.

3.7. Systemic administration of minocycline alleviates damage to the nigrostriatal dopaminergic system in early-stage parkinsonian mice

The presence of M1 microglia and A1 astrocytes may lead to damage of SNc DA neurons; by contrast, A2 astrocytes protect DA neurons from apoptosis following exposure to the neurotoxin MPTP [14,32,39,40]. Our data show that in parkinsonian mice, minocycline reduced the transcription of genes specific to M1 microglia and A1 astrocytes but did not affect the transcription of genes specific to M2 microglia and A2 astrocytes (Figs. 5, 6). We next examined whether systemic minocycline mitigates the damage to the nigrostriatal dopaminergic system in parkinsonian mice. We unilaterally injected 6-OHDA into the MFB of mice and divided the mice into two groups subjected to i.p. injection of either saline or minocycline once per day; mice were sacrificed 3 or 7 days after 6-OHDA injection. We examined the number of SNc neurons immunostained with a TH antibody (Fig. 7a) and the fluorescence intensity in the dorsal striatum after immunostaining with a TH-antibody (Fig. 7c). We observed that minocycline curbed the loss of dopaminergic neurons in the SNc (Fig. 7b) and the loss of dopaminergic fibers and terminals in the dorsal striatum (Fig. 7d) 7 days after 6-OHDA injection. Therefore, minocycline attenuates the 6-OHDA-induced lesion of the nigrostriatal dopaminergic system in early-stage parkinsonian mice.

We then added two parallel groups of mice subjected to i.p. injection of saline or minocycline once per day. We observed that 6-OHDA treatment caused locomotor deficits in the distance traveled and the average velocity in the open-field arena (Fig. 7e,f). Minocycline alleviated these locomotor deficits 7 days after the 6-OHDA injection but did not affect these parameters in control mice (Fig. 7e,f). Similarly, we observed that minocycline mitigated mechanical allodynia on both hind paws in parkinsonian mice 7 days after 6-OHDA injection but did not change the mechanical threshold in control mice (Fig. 7g,h). These results suggest that systemic block of microglia activation may mitigate parkinsonian symptoms during the early stages.

3.8. Minocycline injection in the dorsal striatum mitigates hyperalgesia in early-stage parkinsonian mice

To confirm whether limiting inflammation in the dorsal striatum is sufficient to mitigate motor deficits and hyperalgesia in parkinsonian mice, we next performed daily microinjections of minocycline into the dorsal striatum, starting on the first day after 6-OHDA injection into the MFB (Fig. 8a). Morphological assays confirmed that activation of microglia (Fig. 8b-d) and astrocytes (Fig. 8e-g) was attenuated after 7 daily microinjections (7 days after 6-OHDA injection). We analyzed locomotor behavior and mechanical thresholds in 6-OHDA mice. Unlike systemic administration of minocycline (Fig. 7e,f), striatal injection of

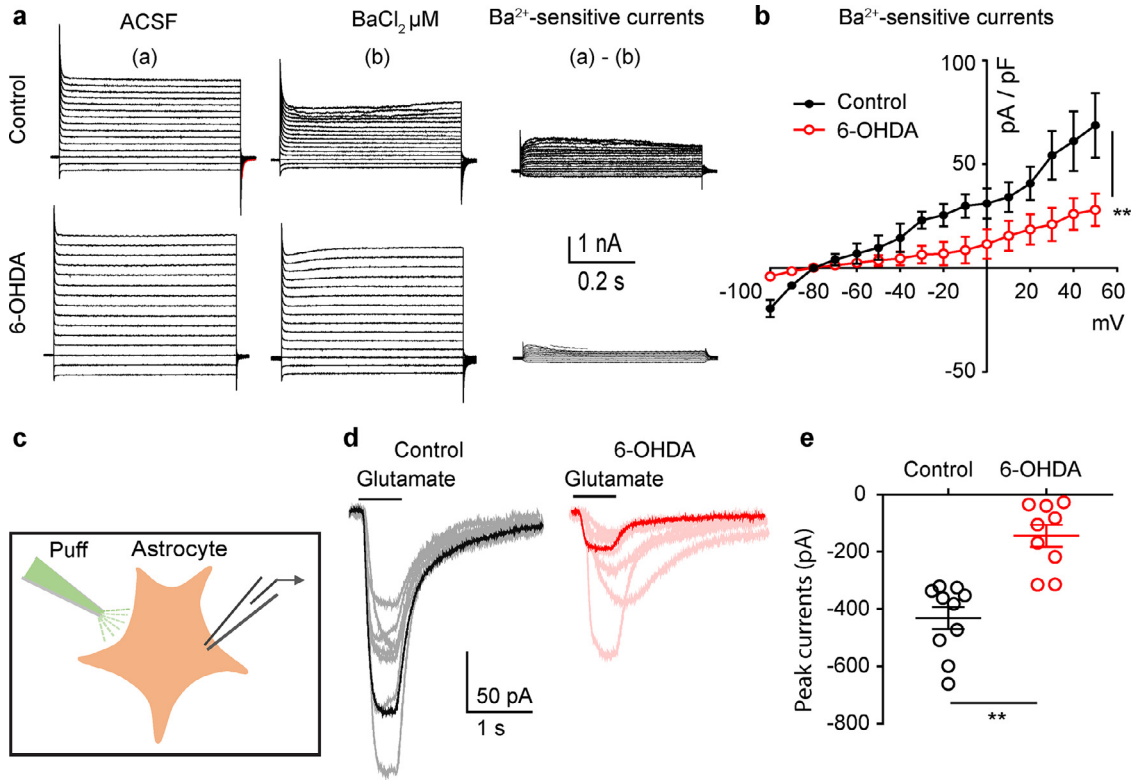

Fig. 4. Alteration of Kir4.1 and glutamate transporters in striatal astrocytes in parkinsonian mice. (a) Barium (Ba^{2+})-sensitive currents were isolated from voltage responses in astrocytes from control and 6-OHDA mice. $n = 8$ astrocytes from 4 mice in each group. (b) I-V curves of the barium (Ba^{2+})-sensitive component in control and 6-OHDA mice. Group: $F_{(1192)} = 31.05$, $P < 0.0001$. Voltage: $F_{(15, 192)} = 11.57$, $P < 0.0001$. (c) Schematic of the patch-clamp recording of glutamate-evoked responses in an astrocyte. (d) Glutamate-evoked traces in control astrocytes (left panel, $n = 10$) and 6-OHDA astrocytes (right panel, $n = 9$) in the presence of 20 μM CNQX and 50 μM APV. The currents are referred to as glutamate transporter currents. (e) Summary of peak amplitudes of the glutamate transporter currents (in (d)) in control and 6-OHDA mice. $t = 5.25$, $P < 0.0001$. Two-way ANOVAs were used for (b). Two-tailed *t*-tests was used for (e). ** $P < 0.01$.

minocycline for 7 days did not change the distance traveled or the average movement velocity in the open-field arena in parkinsonian mice (Fig. 8h,i). However, it did elevate the mechanical threshold in parkinsonian mice with a time course similar to systemically administered minocycline (Figs. 8j,k, and 7g,h).

4. Discussion

Both microglia and astrocytes are implicated in the loss of SNc dopaminergic neurons in PD [13,41]. The activated microglia and astrocytes may be polarized into either inflammatory or neuroprotective phenotypes, which distinctly affect the development of neurodegeneration [42]. In the present study, we addressed how microglia and astrocytes in the dorsal striatum differentiate in parkinsonian mice and affect parkinsonian symptoms. In a hemiparkinsonian mouse model with motor deficits and mechanical allodynia, we observed an increase in activated microglia and reactive astrocytes in the dorsal striatum; the astrocytes exhibited enhanced coupling with other astrocytes, increased voltage-gated potassium currents, and dysfunction in inwardly rectifying potassium channels and glutamate transporters. Our pharmacological intervention experiments demonstrated that blocking the activation of microglia is sufficient to reduce M1 microglia and A1 astrocytes and mitigate motor deficits and mechanical allodynia in parkinsonian mice. Previous studies have shown that the loss of SNc DA neurons and striatal DA axons and terminals, and the subsequent dopamine depletion in the basal ganglia, form the major pathophysiological basis for motor and non-motor symptoms in PD [43]. The present study provides a possible link between neuroinflammation in the dorsal striatum and pain and motor deficits in parkinsonian conditions.

Degeneration of DA axons and terminals occurs earlier than that of the SNc DA neuronal cell bodies [23,24]. Consistent with this, we observed that 6-OHDA injection into the MFB lesioned the nigrostriatal DA system and that the damage to striatal DA axons and terminals was more severe than that to SNc DA neurons in the first 2 weeks after 6-OHDA injection. These hemiparkinsonian mice exhibited bradykinesia and mechanical allodynia, similar to results in previous studies [44]. In parkinsonian mice with overexpressed mutant (A53T) human α-synuclein in the substantia nigra, Chung et al. found that microglia activation and neuroinflammation in the striatum occur before damage to SNc DA neurons [39]. Using qRT-PCR tests of transcription of microglial phenotype-specific genes in the dorsal striatum, we revealed increases in both M1 and M2 microglia 3 and 7 days after 6-OHDA injection, with *Cd86* and *Arg-1* showing the strongest upregulation in M1 and M2 microglia, respectively. These results advance previous reports that activated microglia in the dorsal striatum after 6-OHDA treatment may be polarized into both inflammatory and protective phenotypes, and that *Cd86* and *Arg-1* may be potential markers for these microglia in this parkinsonian mouse model.

We also observed that the number of reactive astrocytes increased in the dorsal striatum 3 and 7 days after 6-OHDA injection, and both *Gfap* and *Lcn2* were upregulated dramatically in reactive astrocytes in the dorsal striatum. Furthermore, A1-specific genes, including *Ggta1, Serping1, Ligp1*, and *H2-D1*, were upregulated in the dorsal striatum. As LCN2 (lipocalin-2) and SERPING1 facilitate apoptosis of neurons [45,46], the increase in the number of A1 astrocytes may have contributed to the loss of DA axons and terminals in the dorsal striatum. Changes were less marked for the A2-specific genes, with only some (including *Cd109* and *Sphk1*) significantly increased 3 and 7 days after 6-OHDA injection. SphK1 (sphingosine kinase 1) binds its receptor, S1P1, and facilitates

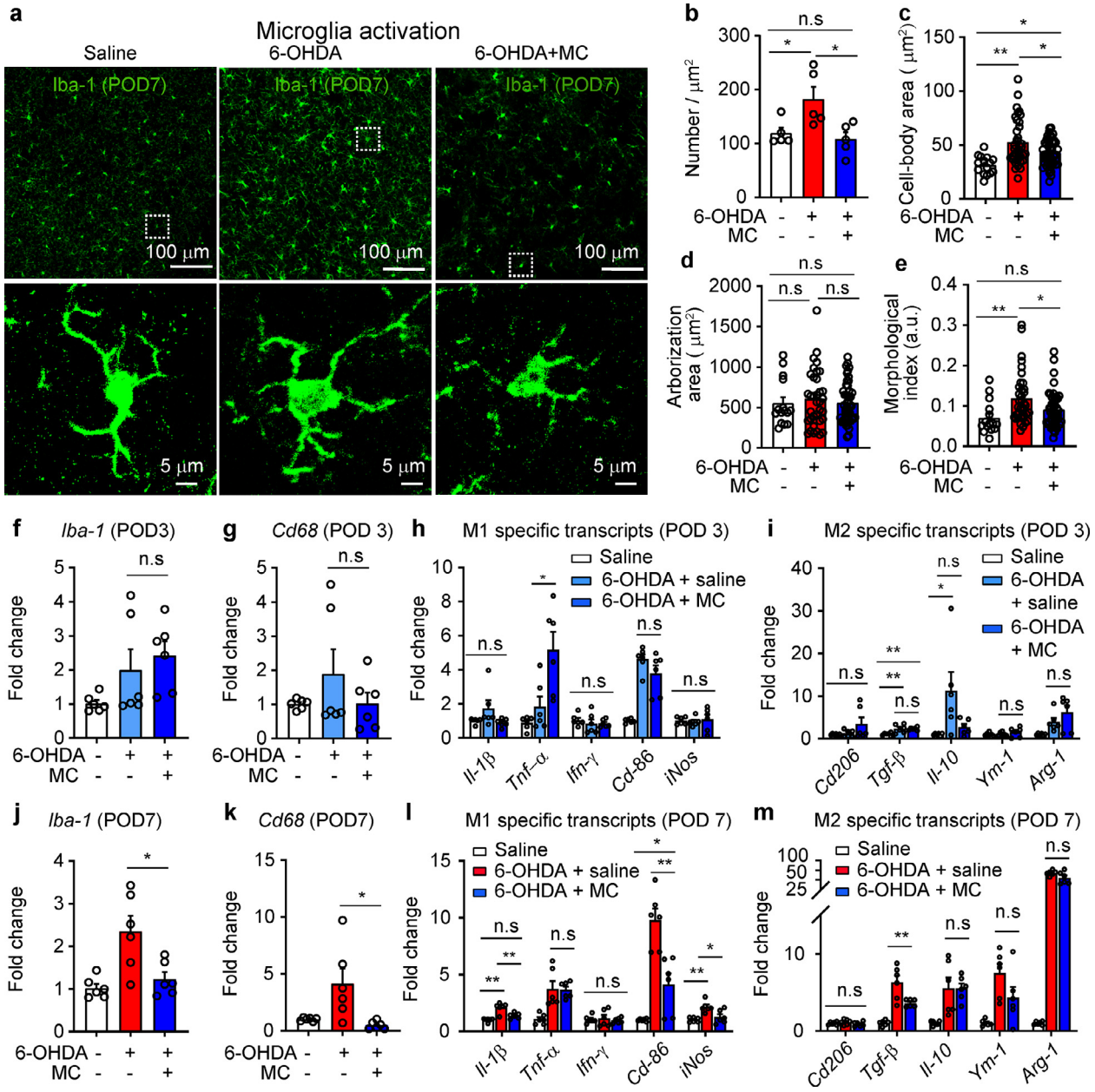

Fig. 5. Minocycline inhibits activation and polarization of striatal microglia in parkinsonian mice. (a) Representative images showing the morphology of Iba-1-positive microglia in saline (MFB injection) + saline (i.p.), 6-OHDA (MFB injection) + saline (i.p.), 6-OHDA (MFB injection) + minocycline (i.p.) (MC) mice. (b-e) Number, cell-body area, arborized area, and morphological index of Iba-1-positive microglia in the striatum in saline ($n = 5$), 6-OHDA ($n = 5$), and 6-OHDA + MC ($n = 5$) mice. (b) Number of microglia, $F_{(2, 12)} = 6.01$, $P = 0.02$. (c) Cell-body area, $F_{(2, 95)} = 10.13$, $P = 0.0001$. (d) Arborized area, $F_{(2, 94)} = 0.34$, $P = 0.71$. (e) Morphological index, $F_{(2, 95)} = 5.37$, $P = 0.006$. (f-i) mRNA level of *Iba-1, Cd68*, M1-microglia-specific genes, and M2-microglia-specific genes in saline, 6-OHDA, and 6-OHDA + MC mice, 3 days after saline or 6-OHDA injection into the MFB. (f) *Iba-1*: $F_{(2, 15)} = 2.82$, $P = 0.09$. $n = 6$ in each group. ((G)) *Cd68*: $F_{(2, 15)} = 1.19$, $P = 0.33$. $n = 6$ in each group. (h) M1-microglia-specific genes: *Il-1β*, $F_{(2, 15)} = 2.57$, $P = 0.11$; *Tnf-α*, $F_{(2, 15)} = 11.56$, $P = 0.0009$; *Ifn-γ*, $F_{(2, 15)} = 0.24$, $P = 0.79$; *Cd86*, $F_{(2, 15)} = 29.64$, $P < 0.0001$; *iNos*, $F_{(2, 15)} = 10.46$, $P = 0.001$; $n = 6$ in each group. (i) M2 microglia-specific genes: *Cd206*, $F_{(2, 15)} = 2.07$, $P = 0.16$; *Tgf-β*, $F_{(2, 15)} = 7.98$, $P = 0.004$; *Il-10*, $F_{(2, 15)} = 4.47$, $P = 0.03$; *Ym-1*, $F_{(2, 15)} = 0.82$, $P = 0.46$; *Arg-1*, $F_{(2, 15)} = 5.89$, $P = 0.01$; $n = 6$ in each group. (j-m) Levels of mRNAs of *Iba-1, Cd68*, M1 microglia-specific genes, M2 microglia-specific genes in saline, 6-OHDA, and 6-OHDA + MC mice, 7 days after saline or 6-OHDA-injection into the MFB. (j) *Iba-1*: $F_{(2, 15)} = 8.97$, $P = 0.03$. (k) *Cd68*: $F_{(2, 15)} = 6.58$, $P = 0.009$. (l) M1 microglia-specific genes: *Il-1β*, $F_{(2, 15)} = 21.67$, $P < 0.0001$; *Tnf-α*, $F_{(2, 15)} = 10.51$, $P = 0.001$; *Ifn-γ*, $F_{(2, 15)} = 0.41$, $P = 0.67$; *Cd86*, $F_{(2, 15)} = 33.86$, $P < 0.0001$; *iNos*, $F_{(2, 15)} = 0.15$, $P = 0.86$; $n = 6$ in each group. (m) M2-microglia-specific genes: *Cd206*, $F_{(2, 15)} = 1.26$, $P = 0.31$; *Tgf-β*, $F_{(2, 15)} = 25.16$, $P < 0.0001$; *Il-10*, $F_{(2, 15)} = 8.48$, $P = 0.003$; *Ym-1*, $F_{(2, 15)} = 9.30$, $P = 0.002$; *Arg-1*, $F_{(2, 15)} = 79.24$, $P < 0.0001$; $n = 6$ in each group. One-way ANOVAs with Bonferroni tests were used for (b-m). * $P < 0.05$; ** $P < 0.01$. n.s, not significant.

GDNF-induced enhancement in the transcription of growth-associated protein 43 (GAP43), a key protein in axons [47]. Because they prevent apoptosis of dopaminergic neurons exposed to MPTP [48], we postulate that activation of A2 astrocytes in the dorsal striatum may attenuate the neurotoxic effects of A1 astrocytes.

Biophysical alterations in astrocytes have been reported after damage to the central nervous system [32]. In the present study, striatal astrocytes in hemiparkinsonian mice exhibited hyperpolarized membrane potentials, higher membrane conductance, and increased membrane capacitance. These correspond to larger voltage-dependent potassium cur-

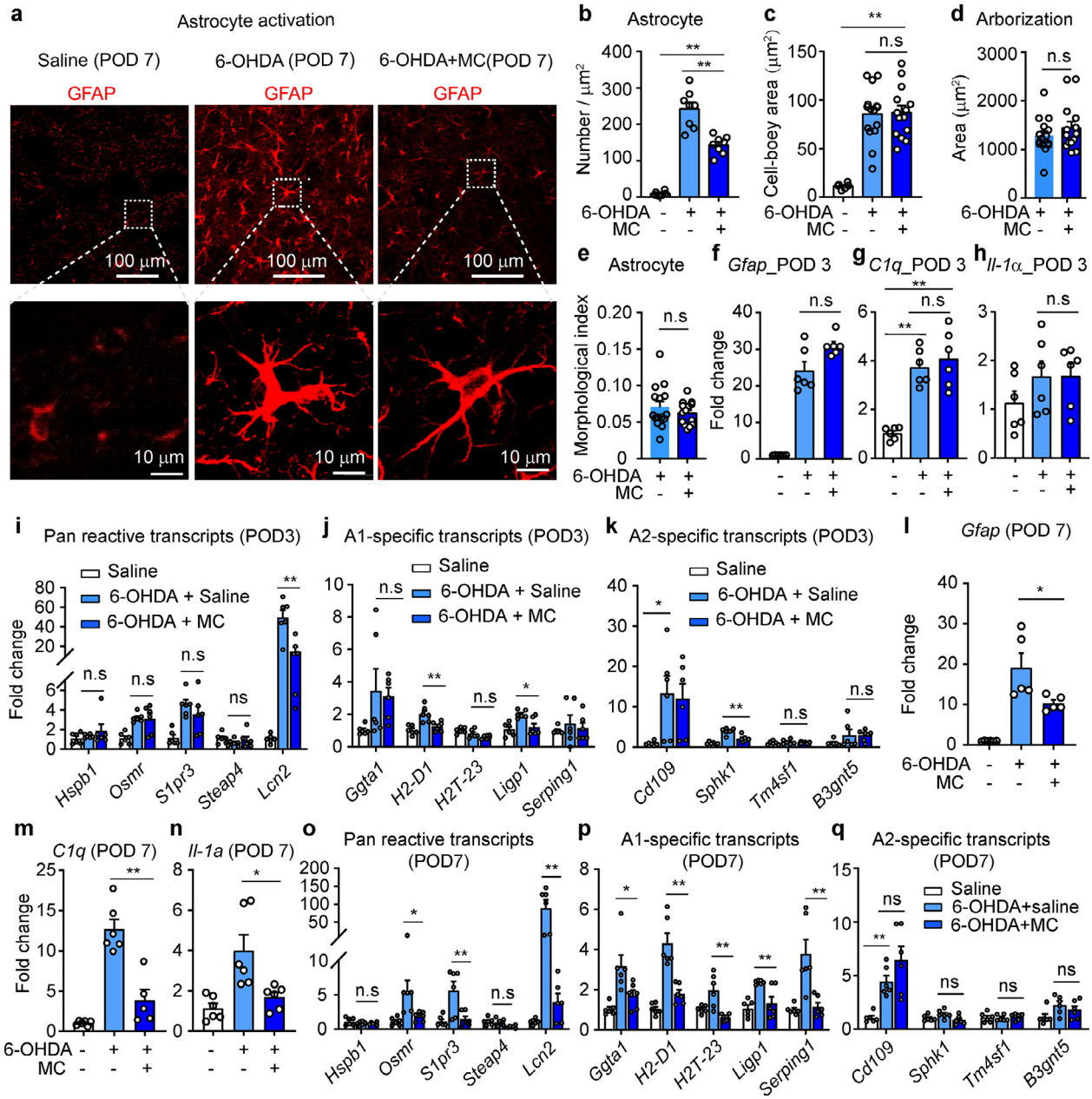

Fig. 6. Minocycline inhibits activation and polarization of striatal astrocytes in parkinsonian mice. (a) Representative images showing the morphology of GFAP-positive astrocytes in saline (MFB injection) + saline (i.p.), 6-OHDA (MFB injection) + saline (i.p.) and 6-OHDA (MFB injection) + minocycline (i.p.) (MC). (b-e) Number, cell body area, arborized area, and morphological index of GFAP-positive astrocytes in the striatum in saline, 6-OHDA, and 6-OHDA + MC mice. (b) Number-Day 7, $F_{(2, 19)} = 76.82$, $P < 0.0001$. (c) Cell-body area-Day 7, $F_{(2, 32)} = 22.75$, $P < 0.0001$. (d) Arborized area-Day 7, $t = 1.01$, $P = 0.32$. (e) Morphological index-Day 7, $t = 0.93$, $P = 0.36$. $n = 15$ sections from 6 mice in each group. (f-k) mRNA level of *Gfap, C1q, Il-1α*, pan-reactive genes, A1-astrocyte-specific genes, and A2-astrocyte-specific genes in saline ($n = 6$), 6-OHDA ($n = 6$), and 6-OHDA + MC ($n = 6$) mice, 3 days after saline or 6-OHDA injection into the MFB. (f) *Gfap*: $F_{(2, 15)} = 102.30$, $P < 0.0001$. (g) *C1q*: $F_{(2, 15)} = 25.78$, $P < 0.0001$. (h) *Il-1α*: $F_{(2, 15)} = 1.37$, $P = 0.28$. (i) Pan-reactive astrocyte genes: *Hspb1*, $F_{(2, 15)} = 0.91$, $P = 0.43$; *Osmr*, $F_{(2, 15)} = 9.82$, $P = 0.002$; *S1pr3*, $F_{(2, 15)} = 9.07$, $P = 0.003$; *Steap4*, $F_{(2, 15)} = 0.91$, $P = 0.42$; *Lcn2*, $F_{(2, 15)} = 23.44$, $P < 0.0001$. (j) A1-astrocyte-specific genes: *Ggta1*, $F_{(2, 15)} = 2.44$, $P = 0.12$; *H2-D1*, $F_{(2, 15)} = 11.77$, $P = 0.0008$; *H2T-23*, $F_{(2, 15)} = 6.63$, $P = 0.0086$; *Ligp1*, $F_{(2, 15)} = 9.15$, $P = 0.003$; *Serping1*, $F_{(2, 15)} = 0.35$, $P = 0.71$; $n = 6$ in each group. (k) A2-astrocyte-specific genes: *Cd109*, $F_{(2, 15)} = 4.20$, $P = 0.04$; *Sphk1*, $F_{(2, 15)} = 29.06$, $P < 0.0001$; *Tm4sf1*, $F_{(2, 15)} = 0.53$, $P = 0.60$; *B3gnt5*, $F_{(2, 15)} = 1.52$, $P = 0.25$; $n = 6$ in each group. (l-q) mRNA level of *Gfap, C1q, Il-1α*, pan-reactive genes, A1-astrocyte-specific genes, and A2-astrocyte-specific genes in saline ($n = 6$), 6-OHDA ($n = 6$), and 6-OHDA + MC ($n = 6$) mice, 7 days after saline or 6-OHDA injection into the MFB. (l) *Gfap*: $F_{(2, 15)} = 21.6$, $P < 0.0001$. (m) *C1q*: $F_{(2, 14)} = 38.67$, $P < 0.0001$. (n) *Il-1α*: $F_{(2, 15)} = 9.45$, $P = 0.002$. (o) Pan-reactive astrocyte genes: *Hspb1*, $F_{(2, 15)} = 1.25$, $P = 0.32$; *Osmr*, $F_{(2, 15)} = 7.33$, $P = 0.0006$; *S1pr3*, $F_{(2, 15)} = 8.89$, $P = 0.003$; *Steap4*, $F_{(2, 15)} = 4.74$, $P = 0.03$; *Lcn2*, $F_{(2, 15)} = 12.75$, $P = 0.0006$. (p) A1-astrocyte-specific genes: *Ggta1*, $F_{(2, 15)} = 9.31$, $P = 0.002$; *H2-D1*, $F_{(2, 15)} = 28.97$, $P < 0.0001$; *H2T-23*, $F_{(2, 15)} = 11.66$, $P = 0.0009$; *Ligp1*, $F_{(2, 15)} = 10.48$, $P = 0.001$; *Serping1*, $F_{(2, 15)} = 12.53$, $P = 0.0006$. (q) A2-astrocyte-specific genes: *Cd109*, $F_{(2, 15)} = 11.46$, $P = 0.001$; *Sphk1*, $F_{(2, 15)} = 3.32$, $P = 0.06$; *Tm4sf1*, $F_{(2, 15)} = 0.19$, $P = 0.83$; *B3gnt5*, $F_{(2, 15)} = 2.97$, $P = 0.08$. Two-tailed unpaired *t*-tests were used for (d,e). One-way ANOVAs with Bonferroni tests (two-tailed) were used for (b,c,f,q). * $P < 0.05$; ** $P < 0.01$; n.s, not significant.

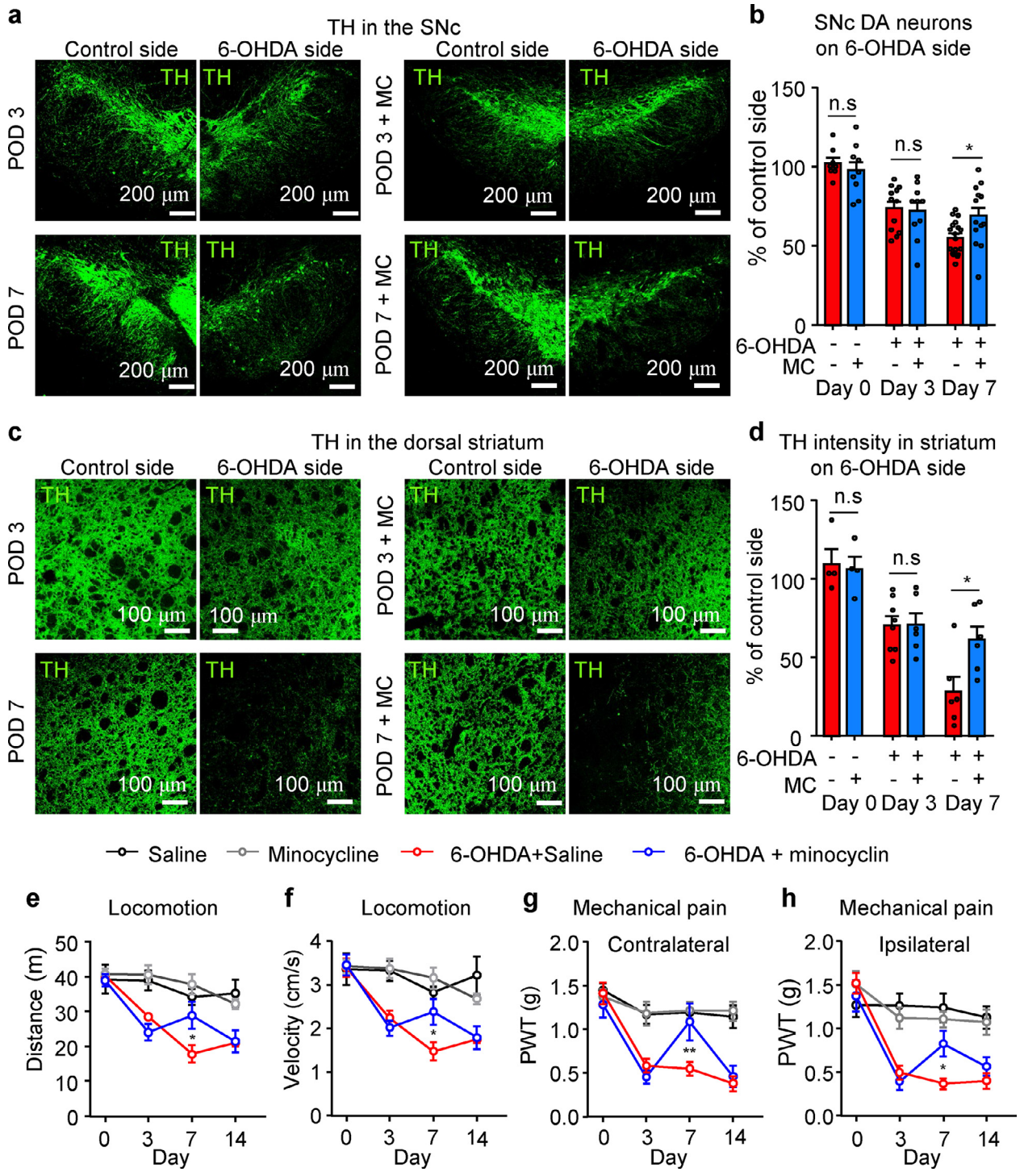

Fig. 7. Systemic minocycline attenuates damage to the nigrostriatal dopaminergic system in parkinsonian mice. (a) Representative TH-antibody-stained images of the substantia nigra from mice sacrificed 3 or 7 days after unilateral 6-OHDA injection into the MFB with or without daily i.p. injections of minocycline (MC). (b) MC reduced the loss of dopaminergic neurons 7 days after 6-OHDA injection. Day 0: $t = 1.59$, $P = 0.13$. 6-OHDA vs 6-OHDA + MC, $n = 10$ sections from 5 mice in each group. Day 3: $t = 0.23$, $P = 0.82$, $n = 11$ sections from 5 mice in each group. Day 7: $t = 2.84$, $P = 0.008$, $n = 15$ sections from 6 mice in each group. Two-tailed *t*-test. (c) Representative TH-antibody-stained images of the dorsal striatum from mice sacrificed 3 or 7 days after unilateral 6-OHDA injection into the MFB with or without daily i.p. injections of MC. (d) MC reduced the loss of dopaminergic fibers and terminals in the dorsal striatum 7 days after 6-OHDA injection. Day 0: $t = 0.28$, $P = 0.79$, $n = 4$ mice in each group. Day 3: $t = 0.04$, $P = 0.97$, $n = 7$ mice in each group, Day 7: $t = 2.61$, $P = 0.03$, $n = 6$ sections from 6 mice in each group. Two-tailed *t*-test. (e) Distance traveled during 20 min in an open-field arena. Interaction, $F_{(9, 99)} = 3.35$, $P = 0.0013$; Time, $F_{(3, 99)} = 15.92$, $P < 0.0001$; Group, $F_{(9, 99)} = 18.41$, $P < 0.0001$. Two-way ANOVA. (f) Averaged movement velocity in an open-field arena. Interaction, $F_{(9, 99)} = 3.38$, $P = 0.0011$; Time, $F_{(3, 99)} = 15.86$, $P < 0.0001$; Group, $F_{(9, 99)} = 17.59$, $P < 0.0001$. (g,h) Mechanical threshold in left and right hind paws. Left side: Interaction, $F_{(9, 128)} = 2.95$, $P = 0.0032$; Time, $F_{(3, 128)} = 14.21$, $P < 0.0001$; Group, $F_{(3, 128)} = 13.88$, $P < 0.0001$. Right side: Interaction, $F_{(9, 120)} = 3.83$, $P = 0.0003$; Time, $F_{(3, 120)} = 20.66$, $P < 0.0001$; Group, $F_{(3, 120)} = 15.65$, $P < 0.0001$. (e-h) $n = 6$ in saline, $n = 10$ in 6-OHDA, $n = 10$ in 6-OHDA+MC, $n = 6$ in MC. Two-way ANOVAs with Bonferroni tests were used. * $P < 0.05$; ** $P < 0.01$; n.s, not significant.

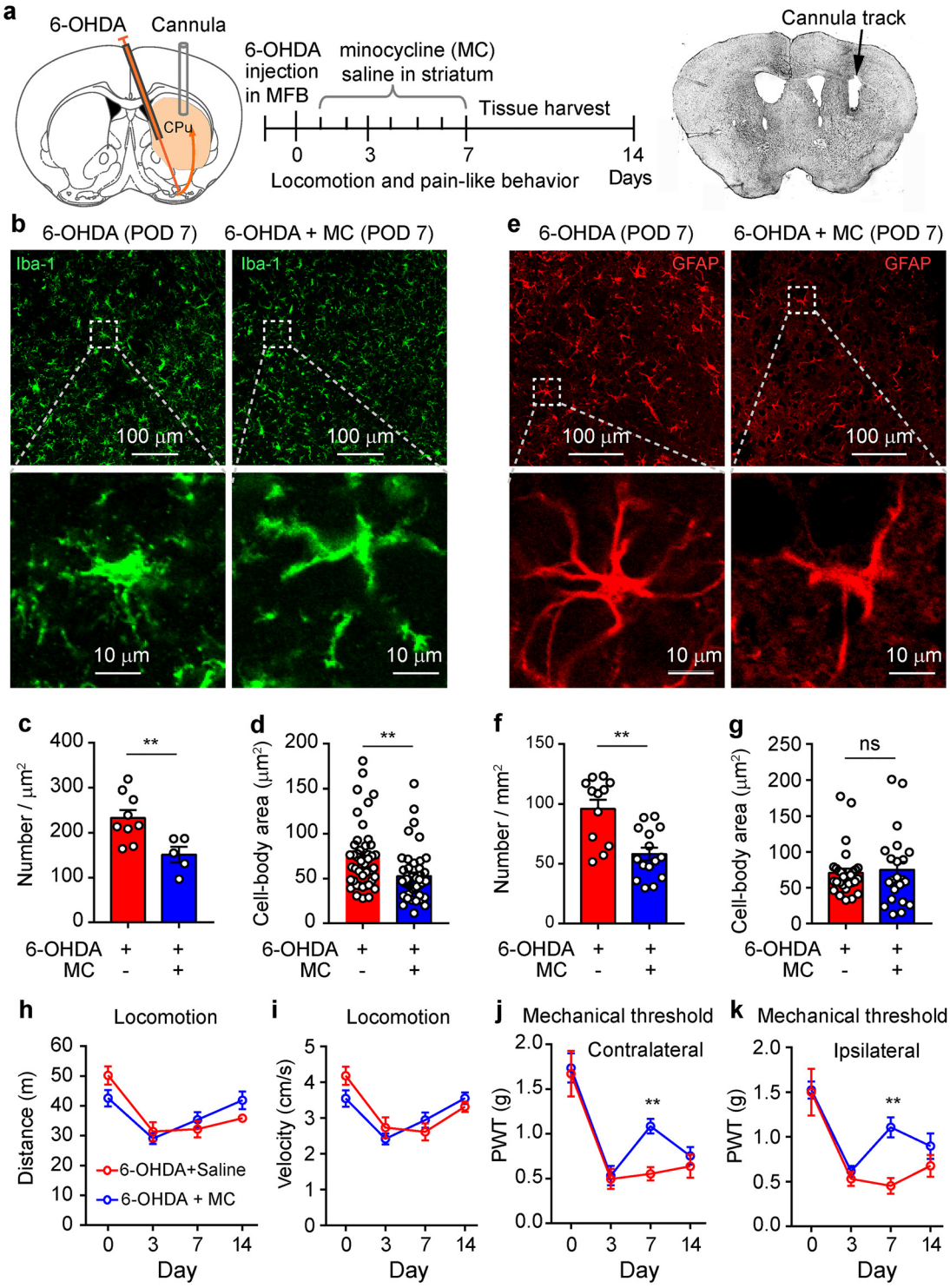

Fig. 8. Minocycline in the dorsal striatum mitigates pain-like behaviors in parkinsonian mice. (a) After 6-OHDA injection and cannula implantation in the dorsal striatum, mice were assigned into two groups for daily microinjection into the dorsal striatum with saline (200 nl) (6-OHDA mice) and minocycline (2 μg in 200 nl) (6-OHDA + MC) for 7 days. Then, mice were subjected to behavioral tests and morphological assays. (b) Representative images showing Iba-1-positive microglia in the dorsal striatum in 6-OHDA and 6-OHDA + MC mice. (c,d) Number and cell-body area of Iba-1-positive microglia from 6-OHDA and 6-OHDA + MC mice. Number: $t = 2.99$, $P = 0.01$, $n = 9$ sections from 6-OHDA mice, $n = 5$ sections from 6-OHDA + MC mice. Cell body: $t = 3.1$, $P = 0.002$, $n = 44$ microglia from 6-OHDA mice, $n = 47$ microglia from 6-OHDA + MC mice. 5 mice in each group. (e) Representative images showing GFAP-positive astrocytes in the dorsal striatum in 6-OHDA and 6-OHDA + MC mice. (f,g) Number and cell-body area of GFAP-positive astrocytes from 6-OHDA and 6-OHDA + MC mice. Number: $t = 4.20$, $P = 0.0003$, $n = 12$ sections from 6-OHDA mice, $n = 15$ from 6-OHDA + MC mice. Cell body: $t = 0.37$, $P = 0.71$, $n = 29$ astrocytes from 6-OHDA mice, $n = 22$ astrocytes from 6-OHDA + MC mice. 5 mice in each group. (h,i) Distance traveled and average velocity over 20 min in the open-field arena before (0 day) and 3, 7, and 14 days after 6-OHDA injection. Distance: Day, $F_{(3, 51)} = 14.3$, $P < 0.001$; Group, $F_{(1, 51)} = 0.01$, $P = 0.92$. (j,k) Mechanical threshold in contralateral and ipsilateral hind paw before (0 day) and 3, 7, and 14 days after 6-OHDA injection. Contralateral: Day, $F_{(3, 51)} = 28.90$, $P < 0.001$; Group, $F_{(1,51)} = 3.37$, $P = 0.07$. Ipsilateral: Day, $F_{(3, 51)} = 22.51$, $P < 0.0001$; Group, $F_{(1, 51)} = 7.38$, $P = 0.009$. Two-tailed t-tests were used in (c,d,f,g). Two-way repeated measures ANOVAs were used in (h-k). $n = 6$ in 6-OHDA, $n = 10$ in 6-OHDA + MC. ** $P < 0.01$.

rents, enhanced astrocyte coupling, and larger cell bodies, respectively. In addition to these changes in biophysical properties, we also observed dysfunction in $Kir_{4.1}$ channels and glutamate transporters in striatal astrocytes in hemiparkinsonian mice. $Kir_{4.1}$ channels and glutamate transporters in astrocytes reuptake extracellular potassium and glutamate, respectively, and are important for the maintenance of the membrane potential and excitability in neurons [49,50]. Thus, dysfunction of $Kir_{4.1}$ channels may contribute to the hyperpolarized membrane potential in striatal astrocytes in parkinsonian mice. Furthermore, the accumulation of extracellular potassium and glutamate may lead to excitotoxicity of striatal DA axons and terminals.

Minocycline specifically inhibits activation of microglia but not astrocytes [51]. Activated microglia release IL-1α and TNF-α, leading to the proliferation of A1 astrocytes [14,21]. In the present study, we observed that daily administration of minocycline over a 7-day period effectively attenuated the increases in M1-specific mRNA but not M2-specific mRNA in hemiparkinsonian mice. Meanwhile, minocycline attenuated the increases in A1-specific mRNA but not A2-specific mRNA. Therefore, in our hemiparkinsonian model, minocycline appears to inhibit the activation of M1 microglia and A1 astrocytes, but not M2 microglia or A2 astrocytes. These anti-inflammatory effects of minocycline may contribute to its protection of SNc DA neurons and striatal DA fibers 7 days after 6-OHDA lesion.

At the behavioral level, systemic administration of minocycline over 7 days mitigated both bradykinesia and mechanical allodynia 7 days after 6-OHDA injection. This result is consistent with the timeline of the effect of minocycline on M1 microglia, A1 astrocytes, and striatal DA fibers. Thus, activation of M1 microglia and A1 astrocytes and loss of striatal DA fibers may contribute to mechanical allodynia in parkinsonian mice within this particular time window. However, although intrastriatal microinjection of minocycline limited neuroinflammation in the striatum and effectively mitigated hyperalgesia, it did not improve bradykinesia. Therefore, extrastriatal inflammatory mechanisms may be involved in bradykinesia in parkinsonian mice. The effects of minocycline on locomotion and mechanical allodynia disappeared by day 14 after 6-OHDA injection. There are at least two possible explanations for this temporary effect of minocycline. First, we only injected minocycline for 7 days: continual minocycline injection may be necessary to maintain its effect. Second, neuroinflammation may contribute to motor dysfunction and pain sensation only in the early stages, thus anti-inflammation may be effective only during this time window. With disease progression, other pathophysiological mechanisms may affect motor control and pain sensation. Therefore, longer-term minocycline administration and more sophisticated pathophysiological studies may be needed to understand the underlying mechanisms.

Although degeneration of the nigrostriatal dopaminergic system and dopamine depletion in the basal ganglia are the major pathophysiological features of PD, systemic pathophysiology may develop, such as hyperactivity in spinal cord dorsal horn neurons [26]. In neuropathic pain following nerve injury, neuronal hyperactivity is accompanied by activation of microglia and astrocytes in the spinal cord [52,53]. Whether neuroinflammation in the spinal cord contributes to hyperalgesia in late-stage parkinsonian mice deserves further investigation.

5. Conclusion

In the present study, we report that 6-OHDA injection into the medial forebrain bundle not only damages the nigrostriatal DA system, leading to motor deficits and mechanical allodynia, but also activates microglia and astrocytes in the dorsal striatum, polarizing them into both inflammatory and neuroprotective phenotypes. Blocking the activation of microglia with minocycline reduced the number of M1 microglia and A1 astrocytes, attenuated the loss of DA neurons in the SNc and DA fibers in the dorsal striatum, and mitigated both motor deficits and mechanical allodynia. This study suggests that anti-inflammatory strategies that target M1 microglia and A1 astrocytes in the dorsal striatum may be effective in slowing down damage to the nigrostriatal DA system and treating parkinsonian symptoms.

CRediT authorship contribution statement

Xue Zhang: Investigation, Formal analysis, Methodology, Validation, Visualization, Writing – original draft. **Zi-Lin Shen:** Formal analysis, Investigation, Resources, Validation. **Ya-Wei Ji:** Formal analysis, Investigation, Resources, Validation. **Cui Yin:** Formal analysis, Investigation, Resources, Validation. **Cheng Xiao:** Conceptualization, Funding acquisition, Methodology, Supervision, Writing – original draft, Writing – review & editing. **Chunyi Zhou:** Conceptualization, Funding acquisition, Methodology, Supervision, Writing – original draft, Writing – review & editing.

Declaration of competing interest

The authors declare that they have no conflicts of interest in this work.

Acknowledgments

This work was supported by the National Natural Science Foundation of China (81971038, 82071231, 82171235, 82271293, 81870891), the Fund for Jiangsu Province Specially-Appointed Professor (C.X., C.Z.), the Natural Science Foundation of Jiangsu Province (BK20211349), and the Leadership Program in Xuzhou Medical University (JBGS202203).

Supplementary materials

Supplementary material associated with this article can be found, in the online version, at doi:10.1016/j.fmre.2023.05.020.

References

[1] B.R. Bloem, M.S. Okun, C. Klein, Parkinson's disease, Lancet 397 (10291) (2021) 2284–2303.
[2] G. Wasner, G. Deuschl, Pains in Parkinson disease–many syndromes under one umbrella, Nat. Rev. Neurol. 8 (5) (2012) 284–294.
[3] D. Aarsland, L. Batzu, G.M. Halliday, et al., Parkinson disease-associated cognitive impairment, Nat. Rev. Dis. Primers 7 (1) (2021) 47.
[4] M.P. Broen, M.M. Braaksma, J. Patijn, W.E. Weber, Prevalence of pain in Parkinson's disease: A systematic review using the modified QUADAS tool, Mov. Disord. 27 (4) (2012) 480–484.
[5] M. Politis, K. Wu, S. Molloy, et al., Parkinson's disease symptoms: The patient's perspective, Mov. Disord. 25 (11) (2010) 1646–1651.
[6] C. Buhmann, J. Kassubek, W.H. Jost, Management of pain in Parkinson's disease, J. Parkinsons Dis. 10 (s1) (2020) S37–S48.
[7] M.J. Armstrong, M.S. Okun, Diagnosis and treatment of Parkinson disease: A review, JAMA 323 (6) (2020) 548–560.
[8] Y. Luan, D. Tang, H. Wu, et al., Reversal of hyperactive subthalamic circuits differentially mitigates pain hypersensitivity phenotype s in parkinsonian mice, Proc. Natl. Acad. Sci. U.S.A. 117 (18) (2020) 10045–10054.
[9] A.D. Ha, J. Jankovic, Pain in Parkinson's disease, Mov. Disord. 27 (4) (2012) 485–491.
[10] I. Morales, A. Sanchez, C. Rodriguez-Sabate, M. Rodriguez, The astrocytic response to the dopaminergic denervation of the striatum, J. Neurochem. 139 (1) (2016) 81–95.
[11] I. Morales, A. Sanchez, C. Rodriguez-Sabate, M. Rodriguez, Striatal astrocytes engulf dopaminergic debris in Parkinson's disease: A study in an animal model, PLoS One 12 (10) (2017) e0185989.
[12] A. Fujita, H. Yamaguchi, R. Yamasaki, et al., Connexin 30 deficiency attenuates A2 astrocyte responses and induces severe neurodegeneration in a 1-methyl-4-phenyl-1,2,3,6-tetrahydropyridine hydrochloride Parkinson's disease animal model, J. Neuroinflamm. 15 (1) (2018) 227.
[13] S.R.W. Stott, R.A. Barker, Time course of dopamine neuron loss and glial response in the 6-OHDA striatal mouse model of Parkinson's disease, Eur. J. Neurosci. 39 (6) (2014) 1042–1056.
[14] S.A. Liddelow, K.A. Guttenplan, L.E. Clarke, et al., Neurotoxic reactive astrocytes are induced by activated microglia, Nature 541 (7638) (2017) 481–487.
[15] H.J. Lee, J.E. Suk, C. Patrick, et al., Direct transfer of α-synuclein from neuron to astroglia causes inflammatory responses in synucleinopathies, J. Biol. Chem. 285 (12) (2010) 9262–9272.
[16] L.A. Cunningham, C. Su, Astrocyte delivery of glial cell line-derived neurotrophic factor in a mouse model of Parkinson's disease, Exp. Neurol. 174 (2) (2002) 230–242.

[17] A. Drinkut, Y. Tereshchenko, J.B. Schulz, et al., Efficient gene therapy for Parkinson's disease using astrocytes as hosts for localized neurotrophic factor delivery, Mol. Ther. 20 (3) (2012) 534–543.
[18] J.L. Zamanian, L. Xu, L.C. Foo, et al., Genomic analysis of reactive astrogliosis, J. Neurosci. 32 (18) (2012) 6391–6410.
[19] Y. Tang, W. Le, Differential roles of M1 and M2 microglia in neurodegenerative diseases, Mol. Neurobiol. 53 (2) (2016) 1181–1194.
[20] M.S. Ho, Microglia in Parkinson's disease, Adv. Exp. Med. Biol. 1175 (2019) 335–353.
[21] S.P. Yun, T.I. Kam, N. Panicker, et al., Block of A1 astrocyte conversion by microglia is neuroprotective in models of Parkinson's disease, Nat. Med. 24 (7) (2018) 931–938.
[22] W. Liu, Y. Tang, J. Feng, Cross talk between activation of microglia and astrocytes in pathological conditions in the central nervous system, Life Sci. 89 (5–6) (2011) 141–146.
[23] H.C. Cheng, C.M. Ulane, R.E. Burke, Clinical progression in Parkinson disease and the neurobiology of axons, Ann. Neurol. 67 (6) (2010) 715–725.
[24] Y. Chu, G.A. Morfini, L.B. Langhamer, et al., Alterations in axonal transport motor proteins in sporadic and experimental Parkinson's disease, Brain 135 (Pt 7) (2012) 2058–2073.
[25] M. Lundblad, B. Picconi, H. Lindgren, et al., A model of L-DOPA-induced dyskinesia in 6-hydroxydopamine lesioned mice: Relation to motor and cellular parameters of nigrostriatal function, Neurobiol. Dis. 16 (1) (2004) 110–123.
[26] D.L. Tang, Y.W. Luan, C.Y. Zhou, et al., D2 receptor activation relieves pain hypersensitivity by inhibiting superficial dorsal horn neurons in parkinsonian mice, Acta Pharmacol. Sin. 42 (2) (2021) 189–198.
[27] C. Zhou, W. Gu, H. Wu, et al., Bidirectional dopamine modulation of excitatory and inhibitory synaptic inputs to subthalamic neuron subsets containing $\alpha4\beta2$ or $\alpha7$ nAChRs, Neuropharmacology 148 (2019) 220–228.
[28] C. Xiao, Y.W. Ji, Y.W. Luan, et al., Differential modulation of subthalamic projection neurons by short-term and long-term electrical stimulation in physiological and parkinsonian conditions, Acta Pharmacol. Sin. 43 (8) (2021) 1928–1939.
[29] T. Wang, G. Xu, X. Zhang, et al., Malfunction of astrocyte and cholinergic input is involved in postoperative impairment of hippocampal synaptic plasticity and cognitive function, Neuropharmacology 217 (2022) 109191.
[30] C. Yin, T. Jia, Y. Luan, et al., A nigra-subthalamic circuit is involved in acute and chronic pain states, Pain 163 (10) (2022) 1952–1966.
[31] L.L. Wang, D. Xu, Y. Luo, et al., Homeostatic regulation of astrocytes by visual experience in the developing primary visual cortex, Cereb. Cortex 32 (5) (2022) 970–986.
[32] S.A. Liddelow, B.A. Barres, Reactive sstrocytes: Production, function, and therapeutic potential, Immunity 46 (6) (2017) 957–967.
[33] A. Volterra, J. Meldolesi, Astrocytes, from brain glue to communication elements: the revolution continues, Nat. Rev. Neurosci. 6 (8) (2005) 626–640.
[34] M.L. Olsen, H. Sontheimer, Functional implications for Kir4.1 channels in glial biology: from K+ buffering to cell differentiation, J. Neurochem. 107 (3) (2008) 589–601.
[35] E. Pajarillo, A. Rizor, J. Lee, et al., The role of astrocytic glutamate transporters GLT-1 and GLAST in neurological disorders: Potential targets for neurotherapeutics, Neuropharmacology 161 (2019) 107559.
[36] T. Tikka, B.L. Fiebich, G. Goldsteins, et al., Minocycline, a tetracycline derivative, is neuroprotective against excitotoxicity by inhibiting activation and proliferation of microglia, J. Neurosci. 21 (8) (2001) 2580–2588.
[37] M. Chen, V.O. Ona, M. Li, et al., Minocycline inhibits caspase-1 and caspase-3 expression and delays mortality in a transgenic mouse model of Huntington disease, Nat. Med. 6 (7) (2000) 797–801.
[38] J. Yrjanheikki, R. Keinanen, M. Pellikka, et al., Tetracyclines inhibit microglial activation and are neuroprotective in global brain ischemia, Proc. Natl. Acad. Sci. U.S.A. 95 (26) (1998) 15769–15774.
[39] C.Y. Chung, J.B. Koprich, H. Siddiqi, et al., Dynamic changes in presynaptic and axonal transport proteins combined with striatal neuroinflammation precede dopaminergic neuronal loss in a rat model of AAV alpha-synucleinopathy, J. Neurosci. 29 (11) (2009) 3365–3373.
[40] D.C. Wu, V. Jackson-Lewis, M. Vila, et al., Blockade of microglial activation is neuroprotective in the 1-methyl-4-phenyl-1,2,3,6-tetrahydropyrid ine mouse model of Parkinson disease, J. Neurosci. 22 (5) (2002) 1763–1771.
[41] P.L. McGeer, E.G. McGeer, Glial reactions in Parkinson's disease, Mov. Disord. 23 (4) (2008) 474–483.
[42] S.J. Miller, Astrocyte heterogeneity in the adult central nervous system, Front. Cell Neurosci. 12 (2018) 401.
[43] P.J. Blanchet, C. Brefel-Courbon, Chronic pain and pain processing in Parkinson's disease, Prog. Neuropsychopharmacol. Biol. Psychiatry 87 (Pt B) (2018) 200–206.
[44] Y. Luan, D. Tang, H. Wu, et al., Reversal of hyperactive subthalamic circuits differentially mitigates pain hypersensitivity phenotypes in parkinsonian mice, Proc. Natl. Acad. Sci. U.S.A. 117 (18) (2020) 10045–10054.
[45] J.H. Kim, O. Kwon, A. Bhusal, et al., Neuroinflammation induced by transgenic expression of lipocalin-2 in astrocytes, Front. Cell Neurosci. 16 (2022) 839118.
[46] M.H. Seo, S. Yeo, Association of increase in Serping1 level with dopaminergic cell reduction in an MPTP-induced Parkinson's disease mouse model, Brain Res. Bull. 162 (2020) 67–72.
[47] M. Murakami, H. Ito, K. Hagiwara, et al., Sphingosine kinase 1/S1P pathway involvement in the GDNF-induced GAP43 transcription, J. Cell. Biochem. 112 (11) (2011) 3449–3458.
[48] J. Pyszko, J.B. Strosznajder, Sphingosine kinase 1 and sphingosine-1-phosphate in oxidative stress evoked by 1-methyl-4-phenylpyrid inium (MPP+) in human dopaminergic neuronal cells, Mol. Neurobiol. 50 (1) (2014) 38–48.
[49] M.L. Olsen, B.S. Khakh, S.N. Skatchkov, et al., New insights on astrocyte ion channels: critical for homeostasis and neuron-glia signaling, J. Neurosci. 35 (41) (2015) 13827–13835.
[50] Y. Zhang, F. Tan, P. Xu, et al., Recent advance in the relationship between excitatory amino acid transporters and Parkinson's disease, Neural Plast. 2016 (2016) 8941327.
[51] M. Tomas-Camardiel, I. Rite, A.J. Herrera, et al., Minocycline reduces the lipopolysaccharide-induced inflammatory reaction, peroxynitrite-mediated nitration of proteins, disruption of the blood-brain barrier, and damage in the nigral dopaminergic syst em, Neurobiol. Dis. 16 (1) (2004) 190–201.
[52] H. Zhao, A. Alam, Q. Chen, et al., The role of microglia in the pathobiology of neuropathic pain development: What do we know? Br. J. Anaesth. 118 (4) (2017) 504–516.
[53] R.R. Ji, A. Chamessian, Y.Q. Zhang, Pain regulation by non-neuronal cells and inflammation, Science 354 (6312) (2016) 572–577.

Chun-Yi Zhou (BRID: 06227.00.39811) received her medical degree and master degree in Science from Xinjiang Medical University, and PhD in pharmacology from University of California, Irvine. Then, she had been trained as a Postdoctoral Scholar and Research Associate in neuroscience in University of Southern California and California Institute of Technology. She joined in the School of Anesthesiology in Xuzhou Medical University as a Professor since 2016. She was a specially appointed professor in Jiangsu Province. Her research has been focusing on neural circuit mechanisms underlying chronic pain as well as the roles of glia-neuron interaction in development and maintenance of chronic pain. She discovered that the subthalamic nucleus in the basal ganglia modulate different pain modality through many downstream pathways, and the hyperactivity of subthalamic neurons and the modifications of their projections contribute to chronic pain in Parkinson's disease, nerve injury, and inflammation.